NTNU
Innovation and Creativity

Modelling and Control of Offshore Ploughing Operations

Thor-Arne Voldsund

Master of Science in Engineering Cybernetics
Submission date: June 2007
Supervisor: Jan Tommy Gravdahl, ITK
Co-supervisor: Jann Peter Strand, Rolls-Royce Marine AS, dept. Control-Aalesund
Morten Breivik, ITK

Norwegian University of Science and Technology
Department of Engineering Cybernetics

Problem Description

Description: The candidate will consider the problem of controlling a marine surface vessel that tows a seabed plough for the purpose of burying pipelines. The following elements must be considered:

1. Set up and present a progress plan for your thesis work so that the due date can be met.
2. What are the existing methods relevant for offshore ploughing operations? What is state-of-the-art industrially?
3. Propose suitable dynamic models of the three major systems that interact in offshore ploughing operations; a seabed plough, a towline, and a marine surface vessel.
4. Review different control schemes that are applicable to the problem under consideration, and select a particular control method based on feasibility of implementation with respect to a readily available suite of sensors, computers, and actuators.
5. Implement the plough, towline, and vessel models as well as the suggested control method in Matlab/Simulink. Simulate a set of relevant ploughing scenarios numerically, and make qualitative comments about the results.
6. If possible, summarize part of the thesis in a paper that is to be presented at a renowned international conference.

Assignment given: 08. January 2007
Supervisor: Jan Tommy Gravdahl, ITK

Summary

In this thesis work, mathematical models required to simulate an offshore ploughing operation has been derived. This includes a surface vessel model, a model of the plough and its friction force due to seabed sediment and a towline model. A Dynamic Positioning control system has been derived in order to regulate the vessel to a desired location based on the plough's desired position. A supervisor module has been derived in order to generate the vessel's reference position in a smooth manner. And finally the total system has been implemented and simulated in the Simulink_TM environment.

The surface vessel model derived in this assignment is based on an offshore supply vessel from the "MatLab Marine GNC Toolbox" in Simulink_TM. The vertical motion of the vessel has been kept constant during simulations, based on the assumption that the buoyancy force of the vessel is large compared to the vertical towline force.

The plough's friction force due to penetration of the seabed sediment has been modeled, based on the content in reference [5], to get a realistic picture of the sediment forces involved in ploughing operations. It was found that the plough's friction force profile changed with different operational boundaries. The boundaries are the ocean depth and the ploughing speed. For the boundaries in this assignment the resulting ploughing force equation were found to be nonlinear and shaped as a sigmoid function.

In this assignment the lumped mass model has been derived for the towline's motion and proven to give reasonably good numerical results when implemented in the Simulink_TM environment. To get a realistic towline motion in seawater, a hydrodynamic quadratic damping force has been added to the equations. This hydrodynamic damping had effect on the towline's tangential and normal motion components.

The DP controller derived in this assignment consists of a PD-controller with feed forward signal from the horizontal towline tension. Feed forward signals are often influenced by noise and must be filtered to obtain low-frequency signals. In this assignment a ordinary 1st-order low-pass filter has been used in order to damp out oscillations from the towline. This filter has been proven to give a good damping effect when the towline was exposed to underwater currents. The DP controller provides good position tracking quality.

The supervisor module designed in this assignment consists of a reference generator an a reference model. The supervisor module is responsible for converting input signals for the plough's desired path into a smooth tracking signal for the vessel's control system. The reference generator produces smaller intermediate reference signals, as input to the reference model, from a final desired vessel position. A circle of acceptance has been introduced in order to change reference values at a convenient vessel location. This has been proven to give a nice effect on the vessel's and the plough's behavior. The reference model has been designed with a speed saturation element, in order to bound the speed of the ploughing operation.

During the case simulations it was found that by defining the operation over a longer distance, a more efficient operation is gained. When crossing longer distances the plough will reach the vessel's speed and underwater current disturbances are small compared to the ploughing force that has gotten time to be built up. Underwater currents has great influence on the towline when the towline's pulling force is small.

In appendix A a CD can be found. On this CD this report can be found, the original work schedule, pictures and the Simulink program for the ploughing operation.

Preface

This thesis has been carried out during the final semester at the Norwegian University of Science and Technology, Trondheim. The thesis is an assignment formulated by Rolls-Royce Marine AS Control Aalesund and has given me the opportunity to learn about modeling and control of offshore ploughing and towing operations. The thesis work has been exciting and time-consuming since it covers a wide range of expertise.

From this work I have learned that a time schedule can easily be forgotten in the amount of work to be done and that the final results not always get to be as good as first planned. I feel that I have learned much about seabed-sediment friction forces, towline cable dynamics and control systems design.

I would like to thank my teacher and supervisor Jan Tommy Gravdahl from the Department of Engineering Cybernetics at NTNU and my supervisors Morten Breivik from Department of Engineering Cybernetics at NTNU and Jann Peter Strand from Rolls-Royce Marine AS Control Aalesund in Aalesund for their support during the whole thesis work. I would also like to thank Vegar Johansen at SINTEF, Eilif Pedersen from the Department of Marine Technology at NTNU and Petter Ottesen from ODIM AS in Aalesund for their support during the modeling work on marine towline cables.

Finally, I would like to thank my family for standing by me during this semester and the five years of study.

Trondheim, July 2007

_____-

Thor-Arne Voldsund

Contents

Summary i

Preface iii

Terminology vii

1 Introduction 1

2 Modeling 5
2.1 System Description and Assumptions 7
2.1.1 Meta System Model 7
2.1.2 System Architecture 9
2.1.3 Assumptions 11
2.2 Mathematical Model of the Surface Vessel 13
2.2.1 Simplified Mathematical Surface Vessel Model 14
2.2.2 Actuators 15
2.3 Mathematical Model of the Plough 17
2.3.1 Simplified Plough Model 17
2.3.2 Derivation of the Plough's Friction Force 19
2.3.3 Analysis of the Plough's Friction Force 25
2.3.4 Resulting Friction Force and Discussion 28
2.4 Mathematical Model of the Towline 30
2.4.1 Lumped Mass Method 31
2.4.2 Choice of Towline 36
2.4.3 Analysis of The Towline Model 38
2.4.4 Initializing the Towline Elements 39
2.4.5 Discussion and Conclusions 43

3 Control Design 45
3.1 Measurement Module 45
3.2 DP Controller 46
3.3 Supervisor Module 47

4 Simulation and Results **53**
4.1 How to Simulate the System in Simulink 53
4.2 Simulation Data 54
4.3 Simulation Case 1: Perfect Operational Conditions 54
4.3.1 Operational Behavior Over a Short Distance Whit Different Circle of Acceptance 55
4.3.2 Operational Behavior Over a Longer Distance 60
4.4 Simulation Case 2: Operational Behavior When the Towline is Exposed to Underwater Current 63

5 Discussion and Conclusion **65**

Bibliography **70**

A CD **71**

Terminology

- COTS : Commercial-Of-The-Shelf.
- DP : Dynamic Positioning.
- DOF : Degrees Of Freedom.
- NED : *N*orth, *E*ast and *D*own (Earth fixed reference frame).
- CG : Center of Gravity.
- mton : Metric Ton.
- PID : Proportional (P), Integral (I), Derivative (D).
- LOS : Line Of Sight.
- INS : Inertial Navigation System.
- GPS : Global Positioning Satellite System.

List of Figures

1.1 Principle sketch of an offshore ploughing operation. 2
1.2 Block diagram of the considered system 3

2.1 Qualitative description of the ploughing operation boundaries. 5
2.2 Meta system model for an offshore ploughing operation. 7
2.3 System architecture for an offshore ploughing operation. 10
2.4 Modular Plough System (MPS) (pipeline mode) found in reference [15]. . 12
2.5 Simplified plough share for the RLP. 12
2.6 3DOF surface vessel model defined in the NED-reference frame 14
2.7 Surface vessel shown in the inertial reference frame. 14
2.8 Offshore supply vessel [12]. 16
2.9 The most common actuators on board a marine DP vessel [11]. 17
2.10 The plough's inertial reference frame (XZ-plane). 18
2.11 Plough share penetrating the seabed sediment. 18
2.12 Pore water pressure profiles as a function of z_{pb} (distance above the plough share bottom) at different plough speed. 21
2.13 The grain crushing force factor, divided by F_0, as a function of the ploughing speed. 27
2.14 The plough's final friction force profile in metric tons. 29
2.15 The towline-elements body fixed reference frame. 32
2.16 Principle sketch of the Lumped Mass Method (xz-plane). 33
2.17 The water flow profile seen in the inertial reference frame. 36
2.18 Elongation of the towline with different damping factors. 39
2.19 XZ-position of the bottom node when the towline swings like a pendulum and the top node has the location ($x_{t,0} = 285m, z_{t,0} = 0m$), (without drag forces). 40
2.20 XZ-position of the bottom node when the towline swings like a pendulum and the top node has the location ($x_{t,0} = 285m, z_{t,0} = 0m$), (with drag forces). 40
2.21 The shape of a Catenary curve. 42
2.22 Manual placement of towline elements. 43
2.23 Experimental initialization of the towline elements vs the Catenary equation. 44

3.1 Total system overview. 46

3.2 Ploughing path in the XY-plane (horizontal plane). 49
3.3 The vessel's reference points toward the final reference r_v. 50
3.4 Transforming the plough's desired position into incremental reference step values for the vessel's position. 51

4.1 The vessel's and plough's position vs their desired position and reference ($R0 = 0$ and $r_p = -250m$). 56
4.2 The vessel's and plough's position vs their desired position and reference ($R0 = 0.25$ and $r_p = -250m$). 56
4.3 The vessel's and plough's speed ($R0 = 0$ and $r_p = -250m$). 57
4.4 The vessel's and plough's speed ($R0 = 0.25$ and $r_p = -250m$). 57
4.5 Control force and horizontal towline forces ($R0 = 0$ and $r_p = -250m$). . . 58
4.6 Control force and horizontal towline forces ($R0 = 0.25$ and $r_p = -250m$). 58
4.7 Elongation of the towline ($R0 = 0$ and $r_p = -250m$). 59
4.8 Elongation of the towline ($R0 = 0.25$ and $r_p = -250m$). 59
4.9 The vessel's and plough's position vs their desired position and reference ($R0 = 0.25$ and $r_p = 0m$). 61
4.10 The vessel's and plough's speed ($R0 = 0.25$ and $r_p = 0m$). 61
4.11 Control force and horizontal towline forces ($R0 = 0.25$ and $r_p = 0m$). . . . 62
4.12 Elongation of the towline ($R0 = 0.25$ and $r_p = 0m$). 62
4.13 The system's initial and final states ($R0 = 0.25$ and $r_p = 0m$). 63
4.14 Control force and horizontal towline forces (with underwater current). . . 64

A.1 CD content. 71

List of Tables

2.1 Plough and sediment data used in the case study when comparing $F_{0,grc}$ with $F_{0,cav}$. 27
2.2 Towline Cable Data. 38

4.1 Simulation data common for all case scenarios. 54

Chapter 1

Introduction

Offshore ploughing operations are carried out by many companies all over the world. The main purpose of such operations are to bury pipelines into the seabed, for protection against fishing activities, anchor movement and other moving obstacles on the seabed. Underwater pipelines are used to transport oil and gas from offshore oil and gas fields. Hydro's Ormen Lange project is a good example where gas is to be transported in pipelines at the ocean bottom between Nyhamna in Norway and Easington in the United Kingdom [16]. The pipeline, which is called Langeled, has at the most a diameter of 1 metre. Before the ploughing operation can begin, the pipelines are laid on the seabed by a pipe-laying vessel, see reference [7]. When burying pipelines at large water depths, a surface vessel is often required for towing the so-called pipeline plough (from now on it is only called a plough), see the principle sketch in Figure 1.1.

This thesis assignment is formulated by Rolls-Royce Marine AS Control-Aalesund and will focus on modeling, simulation, and control-design and simulation of an offshore ploughing operation. In Figure 1.1, four elements are to be mathematically modeled:

1 The surface vessel, which is controlled by a Dynamic Positioning (DP) system.

2 The plough, which is responsible for burying the pipeline at a constant depth into the seabed.

3 The towline, which is used by the surface vessel to tow the plough.

4 The seabed sediment, which is the main contribution to the friction forces acting on the plough.

When designing controllers for ploughing operations, a good mathematical model of the plough and the friction force has to be derived to obtain good transient motion behavior. This is because the model can be used as a feed-forward part in the controller. To derive such models one has to obtain realistic data for a real-life plough and seabed sediment data. The size, shape and weight of the plough and the shape of its plough-share will give the answers to the friction forces acting on it.

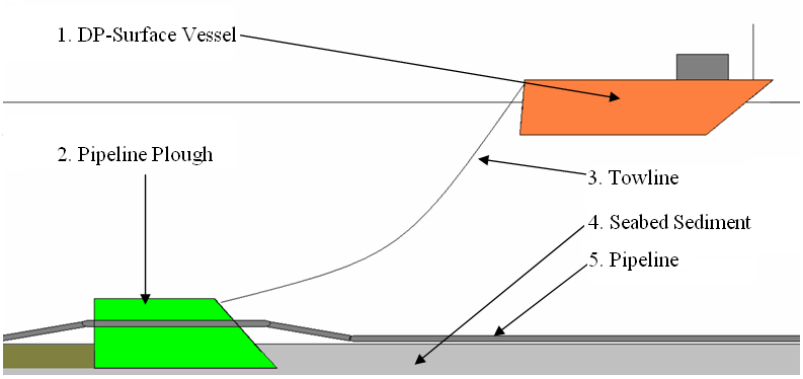

Figure 1.1: Principle sketch of an offshore ploughing operation.

Because of the large friction force acting on the plough from the seabed sediment, big ploughs are towed by surface vessels with powerful propulsion systems. Due to changes in the density of the seabed sediment, the tension in the towline will vary. Normally there is an active tension control system for the towline installed on board the surface vessel. This tension control system consists of hydraulic servomotors and tension measurement units attached to a set of towline reels. This system will pull in or pay out a specified towline length depending on whether the tension in the towline decreases or increases respectively. The main objective for this tension control system is to maintain a constant tension in the towline to avoid breaking it and to avoid large damages to the pipeline, plough and the surface vessel. By having an active tension control system, the bandwidth for controlling the towline is increased in that it is not dependent of the low-frequency control of the surface vessel. In this assignment a towline tension control system will not be implemented.

By assuming that the surface vessel has a DP-control system on board, exploitation of this system must be made to gain control of the towline tension and the plough. This requires derivation of the following mathematical models:

- A model of the surface vessel and its external forces due to weather conditions.
- A model of the plough and its external friction force.
- A model of the towline and its external forces.

The total system can be illustrated as in Figure 1.2. It is assumed that a model-based DP-controller is readily available for the surface vessel. A supervisor module that calculates the relevant reference signals that obtain ploughing capability, and feeds them to the commercial-of-the-shelf (COTS) DP-controller, must be designed.

The mathematical model of the plough has to be derived for simulation of its motion and possibly for the use as a feed-forward part in the supervisor module. A real plough

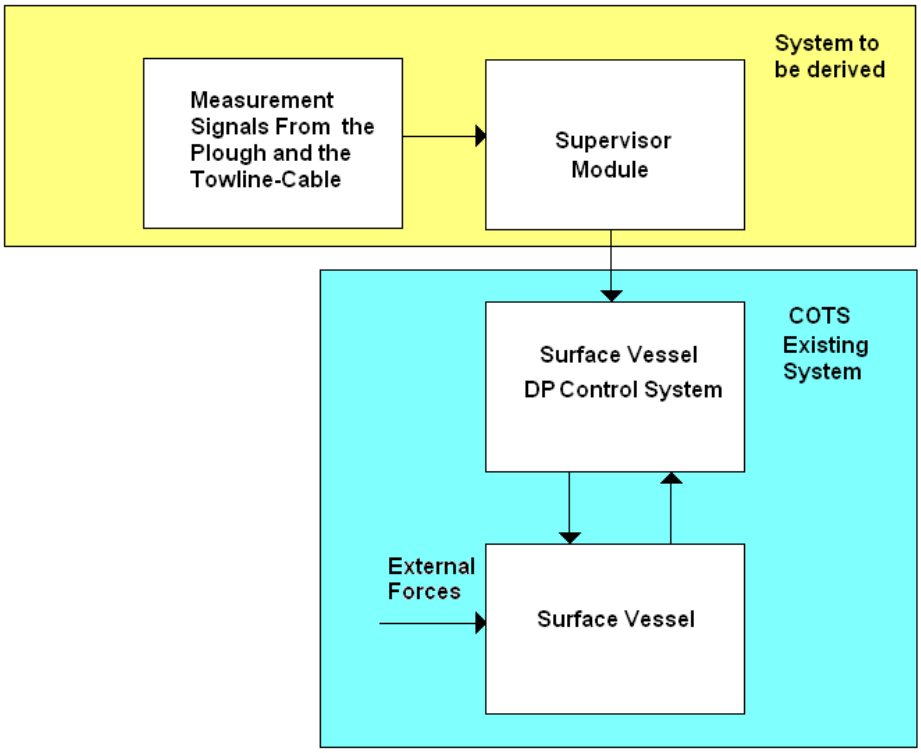

Figure 1.2: Block diagram of the considered system

must be used as a basis for deriving such a model. The external friction force acting on the plough must also be modeled. The main contribution to this external force is the force from the seabed sediment applied to the plough as it penetrates the sediment.

The towline must be strong enough to manage the large forces due to towing of the plough. An accurate model of the towline is therefore needed to generate realistic force vectors. There are several methods for modeling the towline. The model is usually derived by dividing the towline into several finite elements. The choice of method depends on the water depth and the choice of computer simulation system. At large water depths a great number of finite elements must be considered. This great number of elements can give raise to large computation time. If the number of elements is reduced, a great amount of deviation from the real towline curvature can arise.

The supervisor module is meant to be a higher level of control for the DP-controller. Its main task is to feed the DP-controller with the desired reference signals for the surface vessels position, speed and acceleration. Since the DP-controller is COTS, it may require adjustments to gain the correct responses to the varying towline tension. The DP-controller, along with the propulsion system of the vessel, is needed to make sure that the tension in the towline is kept at a desired level so that the plough is kept on track under the whole operation.

Chapter 2

Modeling

Simulators are often used for simulation of real-life marine-systems before installation and sea trial. Unexpected events, operational boundaries and physical requirements are then discovered and can be compensated for. Economical loss can be avoided.

An offshore ploughing operation simulator requires a good mathematical model of the plough, the towline and the surface vessel. Mathematical models of the environmental forces like wind, waves, sea-currents and seabed-sediment friction forces are also required. When deriving these mathematical models, simplifications can be made by giving a qualitative description of the ploughing operation boundaries. These boundaries can be illustrated as in Figure 2.1. Inside the sphere, in Figure 2.1, one can assume that the weather is nice, that the operational path trajectory is straight and that the speed is low.

In chapter 2.1 the total system and necessary assumptions are described for an offshore ploughing operation. In chapter 2.2 a mathematical model of the surface vessel is derived for low-speed and in chapter 2.3 a mathematical model of the plough and the seabed-sediment friction force is derived. The friction force is simulated for a given plough and

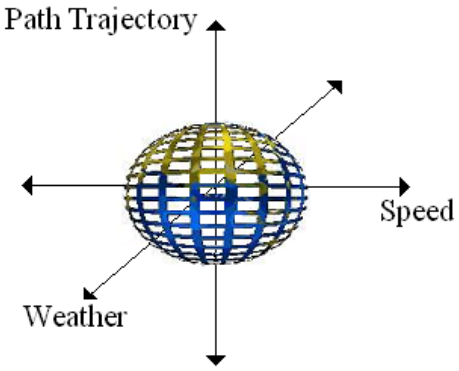

Figure 2.1: Qualitative description of the ploughing operation boundaries.

a given sediment type. In chapter 2.4 a mathematical model of the towline is derived.

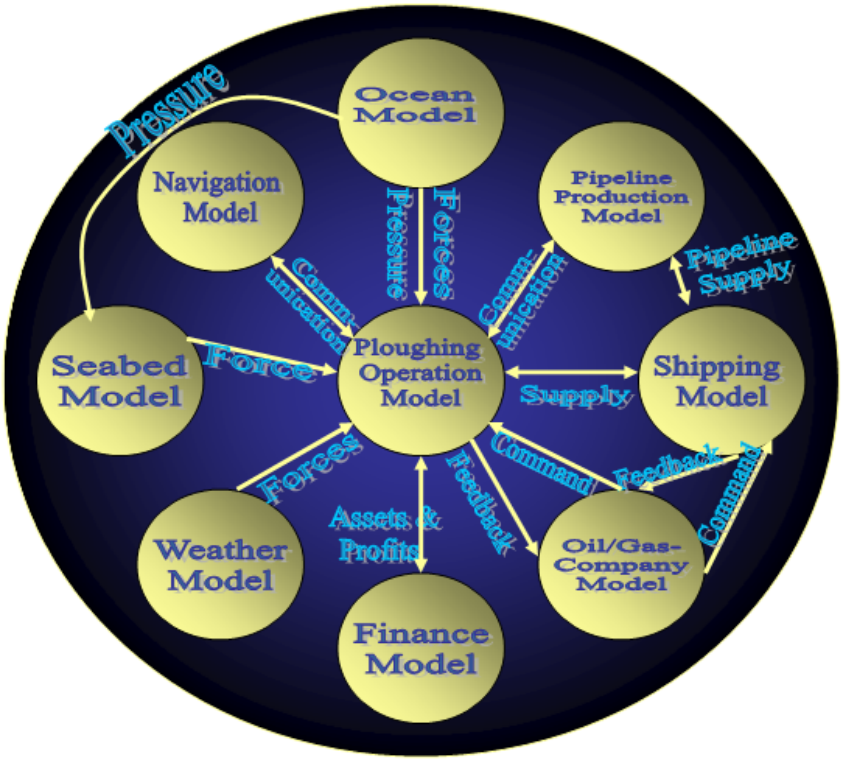

Figure 2.2: Meta system model for an offshore ploughing operation.

2.1 System Description and Assumptions

2.1.1 Meta System Model

To get a total system overview one has to set up a meta system model, see Figure 2.2. This system describes the different models involved in a ploughing operation. Not all models in the meta system model will be covered in the modeling process for this assignment. The different models in the meta system model will be explained below.

Description of the Meta System Model

Ocean Model:

- *Purpose:* The purpose of this model is to give a realistic picture of ocean waves and currents that will influence the vessels and the towlines motion. It is also to give a realistic picture of the water pressure acting on the plough and the seabed soil.

- *Connection:* This model has a connection to the seabed-model in terms of pressure due to the ocean height. It also has a connection to the Ploughing operation model

in form of pressure on the plough and the towline and in terms of wave/current forces on the surface vessel.

Navigation Model:

- *Purpose:* The purpose of this model is to measure the position of the surface vessel.
- *Connection:* This model has a connection from the GPS-satellite-navigation system to the surface vessel, through frequency communication.

Seabed Model:

- *Purpose:* The purpose of this model is to give a realistic measure of the seabed friction force acting on the plough model.
- *Connection:* This model has a connection to the plough model in terms of force. The model also has a connection to the ocean model in terms of water pressure on the seabed-sediment.

Weather Model:

- *Purpose:* The purpose of this model is to give a realistic measure of the weather acting on the surface vessel.
- *Connection:* This model has a connection to the surface vessel through a weather sensor-model.

Ploughing Operation Model:

- *Purpose:* The purpose of this model is to give a realistic picture of what type of surface vessel and towline that is needed for a ploughing operation. It depends on, for example, the size of the plough, the ocean depth and the friction force from the seabed-sediment. This model is also to provide a realistic picture of the dynamic between the plough and the surface vessel.
- *Connection:* This model has a connection to the seabed model, the navigation model, the ocean model and the weather model.

The models which will be further studied are the seabed model and the ploughing operation model. The other models in the meta system model will not be discussed any further; one only has to know that they are present. The system architecture of the ploughing operation model will be described in the next subsection.

2.1.2 System Architecture

The relationship between the vessel, towline and plough is shown in Figure 2.3. The environmental influences are also shown. Below follows a description of the system architecture.

Description of the System Architecture

Plough Model:

- *Purpose:* The purpose of this model is to bury pipelines into the seabed. It is to maintain a constant ploughing depth and a steady course to keep the pipelines from being damaged.
- *Connection:* This model is directly connected to the towline. It is also connected to the ocean-model in term of pressure and the seabed model in terms of seabed friction forces. And it is directly connected to the pipeline.

Towline Model:

- *Purpose:* The purpose of this model is to connect the surface vessel to the plough. It is to have some dynamic in case the plough runs into high density seabed-sediment like rocks or other hard sediment material.
- *Connection:* This model is directly connected to the surface vessel and the plough. It is also connected to the ocean-model in term of pressure and current acting on the towline. This is assumed to be disturbances.

Surface Vessel Model:

- *Purpose:* The purpose of this model is to control the motion of the plough. The plough is to follow a specified route determined by the position of the pipeline. The surface vessel must pull the plough in the desired direction. The surface vessel must also maintain a correct heading and course.
- *Connection:* This model is connected to the navigation-model which measures the exact location of the surface vessel. The surface vessel model is also connected to the weather model which measures the wind direction and strength. Other disturbances comes from the ocean model. This is the wave height and the wave and current directions. The surface vessel model is directly connected to the towline. Finally the surface vessel model has a communication line to the plough. The plough tells the surface vessel its position, speed, direction and other possible information that the surface vessel requires to control the plough.

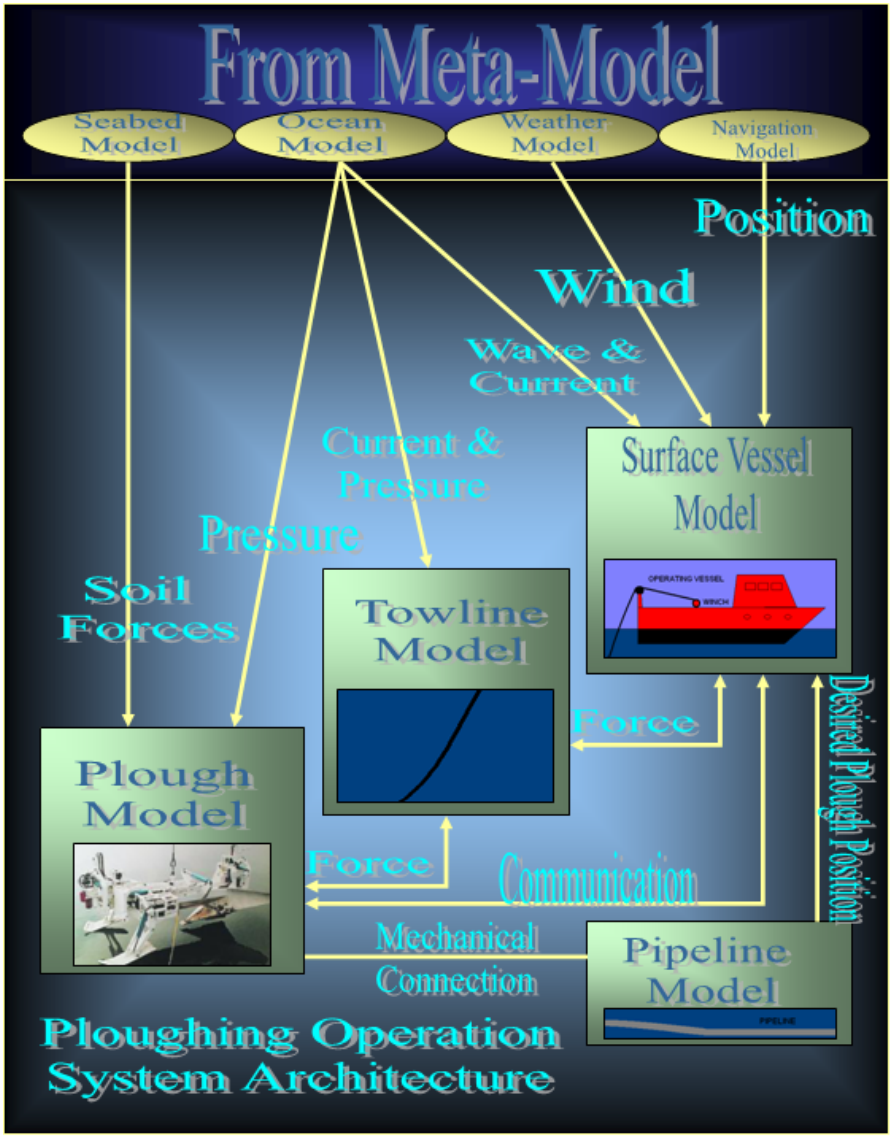

Figure 2.3: System architecture for an offshore ploughing operation.

2.1.3 Assumptions

Assumptions About the Ploughing Operating Conditions

- No wind.
- No currents.
- No waves.
- According to [22], the speed of an offshore ploughing operation can be between $0.003m/s$ and $0.16m/s$. The velocity depends on the seabed sediment and the ploughing depth. The speed must be low when the seabed sediment is hard. In reference [3] the performance of pipeline ploughs in layered soils is analyzed with a ploughing speed set to $0.05m/s$. In the cost analysis for waste disposal of scrap pipelines, [20], the average ploughing operation velocity is set to $0.05m/s$. This is low-speed maneuvering according to [10]. The above statements justifies that the offshore ploughing velocity in this assignment can be between $0m/s$ and $0.16m/s$.
- The operation path trajectory is straight (i.e., the significant motion direction is surge).
- Using only low-frequency models.
- According to [22], the maximum ocean depth for ploughing in the North Sea is $200m$ and the average ocean depth is $70 - 140m$. The absolute maximum ocean depth worldwide is $1000m$. This is due to the limitations on the electronic equipment connected to the plough, i.e. video camera etc. The above statements justifies that the ocean depth in this assignment can be between $70m$ and $200m$.
- Density of seawater (sw): $\delta_{sw} = 1025\frac{kg}{m^3}$

Assumptions About the Plough

- Assuming the weight of seawater has no effect on the ploug's normal force due to small plough-surface.
- Disregarding hydrodynamic added mass (Water put in motion due to the motion of the plough) due to the simple shape of the plough.
- Assuming that the real life plough (RLP) has the same specification as the Modular Plough System (MPS) (pipeline mode) found in reference [15], see Figure 2.4.
- Assuming there exists a simplified plough share for the RLP, see Figure 2.5.
- When modeling the RLP's dynamic, the weight of the pipeline that penetrates the plough is disregarded.

Figure 2.4: Modular Plough System (MPS) (pipeline mode) found in reference [15].

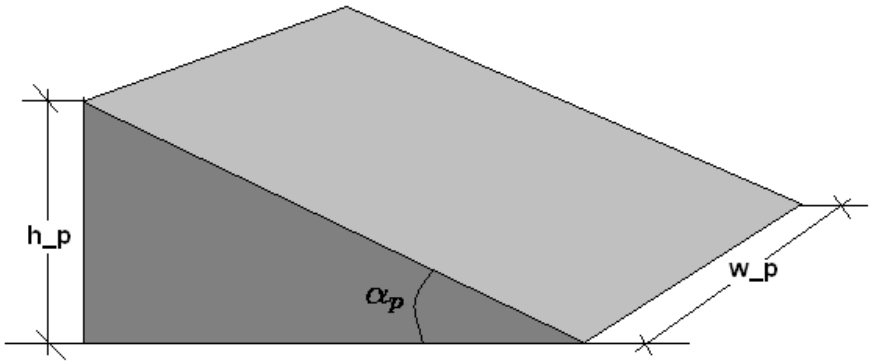

Figure 2.5: Simplified plough share for the RLP.

- The RLP's specification is approximately according to reference [15] as follows:

$m_p = 52000Kg$	- The RLP's weight (submerged).
$w_p = 0.5m$	- The plough share width.
$h_p = 1.5m$	- The plough share height.
$\alpha_p = 30degree$	- The plough share angle.
$H_{sea,max} = 1000m$	- The RLP's maximum operating depth.

Assumptions About the Towline

- Neglect bending stiffness and torsional stiffness. This means that only axial stiffness will be considered.
- The cross-sectional area of the towline will not undergo significant change due to axial deformation of the towline.

2.2 Mathematical Model of the Surface Vessel

To maneuver the surface vessel during the ploughing operation a dynamic positioning (DP) system is utilized. DP systems have traditionally been a $low - speed$ application (max $1m/s$), where the DP functionality is either to keep a fixed position and heading or to move slowly from one location to another (marked position). DP also have the functionality of specialized tracking for pipe-layers or towing-vessels which is the case in this project, see reference [11]. From reference [11] a 3DOF rigid body model for low speed horizontal motion is already derived as follows:

$$\dot{\eta} = R(\psi)\nu \tag{2.1}$$

$$M\dot{\nu} + D\nu = \tau \tag{2.2}$$

where η is the vessel's position and orientation vector in the NED-reference frame (see Figure 2.6):

$$\eta = \begin{bmatrix} n & e & \psi \end{bmatrix}^T, \tag{2.3}$$

ν is the vessel's linear and angular velocity:

$$\nu = \begin{bmatrix} u & v & r \end{bmatrix}^T, \tag{2.4}$$

$R(\psi)$ is the rotation matrix about the vessel's vertical axis which transforms the vessel-fixed velocity vector into the earth-fixed velocity vector:

$$R(\psi) = \begin{bmatrix} cos\psi & -sin\psi & 0 \\ sin\psi & cos\psi & 0 \\ 0 & 0 & 1 \end{bmatrix}, \tag{2.5}$$

M is the vessel's mass matrix:

$$M = M_{RB} + M_A = \begin{bmatrix} m & 0 & 0 \\ 0 & m & mx_g \\ 0 & mx_g & I_z \end{bmatrix} + \begin{bmatrix} -X_{\dot{u}} & 0 & 0 \\ 0 & -Y_{\dot{v}} & -Y_{\dot{r}} \\ 0 & -Y_{\dot{r}} & -N_{\dot{r}} \end{bmatrix}$$

$$= \begin{bmatrix} m - X_{\dot{u}} & 0 & 0 \\ 0 & m - Y_{\dot{v}} & mx_g - Y_{\dot{r}} \\ 0 & mx_g - Y_{\dot{r}} & I_z - N_{\dot{r}} \end{bmatrix}, \tag{2.6}$$

D is the vessel's linear damping matrix due to laminar skin friction:

$$D = \begin{bmatrix} -X_u & 0 & 0 \\ 0 & -Y_v & -Y_r \\ 0 & -N_v & -N_r \end{bmatrix}, \tag{2.7}$$

and τ is the vessel's control forces and moments:

$$\tau = \begin{bmatrix} X & Y & N \end{bmatrix}^T. \tag{2.8}$$

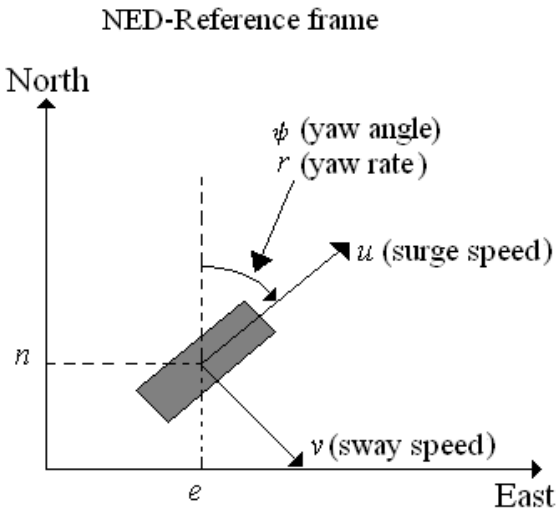

Figure 2.6: 3DOF surface vessel model defined in the NED-reference frame

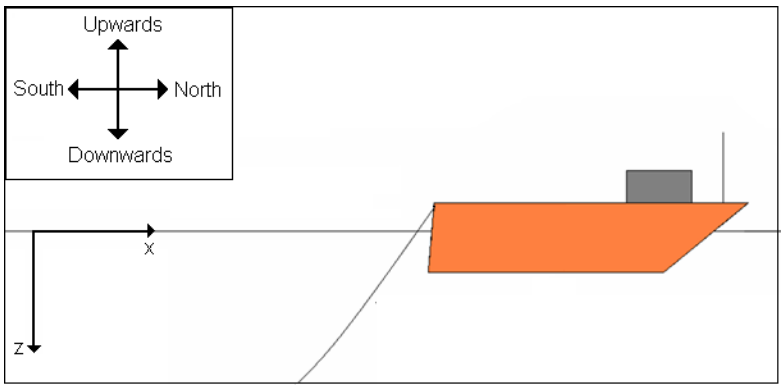

Figure 2.7: Surface vessel shown in the inertial reference frame.

2.2.1 Simplified Mathematical Surface Vessel Model

The main motion component for the surface vessel is surge. The 3DOF motion model described above can therefore be simplified to only account for this motion. Another simplification made is that the surface vessel is only moving in the north/south direction with a displacement x_v relative to the inertial reference frame (which is the same as the NED-reference frame). The inertial (global fixed) reference frame (X, Z), which in the NED-reference frame is called $(North, Down)$ respectively, is defined with the origin located at the mean surface where X is the horizontal direction defined positive to the north and Z is the vertical direction defined positive downwards. In Figure 2.7 the vessel is shown in the inertial reference frame. The surge equation is according to the 3DOF

model as follows:

$$\dot{x}_v = u_v \tag{2.9}$$
$$m_v \dot{u}_v = \tau_x - d_v u_v - F_{t,x} \tag{2.10}$$

where $\dot{x}_v = u_v$ is the surge speed, $m_v = (m - X_{\dot{u}})$ is the vessel's mass and added mass, τ_x is the vessel's control force in the surge direction, $d_v = -X_u$ is the vessel's linear damping due to skin friction and $F_{t,x}$ is the towline tension in the x-direction. The angle ψ, in the rotation matrix from equation 2.5, is zero since the vessel is headed north.

The surface vessel used in this project is the offshore supply vessel 'Northern Clipper' shown in figure 2.8. From the 'MatLab Marine GNC Toolbox' in Simulink_TM the following data were found for the offshore supply vessel:

$d_v = 50242kg/s$ -Linear damping
$m_v = 5312200kg$ -The vessel's mass and added mass

The vessel's time constant can be computed as follows according to [11]:

$$T_v = \frac{m_v}{d_v} = 105.7s \tag{2.11}$$

and the vessels natural frequency becomes:

$$\omega_{n,v} = 1/T_v = 0.0095 \tag{2.12}$$

When disregarding the nonlinear towline force ($F_{t,x}$) in equation 2.10 the vessel model becomes linear, and the transfer function can be written in the following form:

$$H_v(s) = \frac{x_v}{\tau_x} = \frac{1}{d_v s(T_v s + 1)} \tag{2.13}$$

The vessels eigenvalues are found as follows:

$$\frac{1}{d_v s(T_v s + 1)} = 0 \Rightarrow \tag{2.14}$$
$$\lambda_1 = 0 \tag{2.15}$$
$$\lambda_2 = -\frac{1}{T_v} = -0.00946 \tag{2.16}$$

This means that the vessel is asymptotically stable.

2.2.2 Actuators

DP surface vessels normally use more than one actuator to maintain their position and heading. These actuators can be configured to produce the desired force and moment needed, and at the same time optimize the fuel consumption for the vessel. The listed actuators below are the most common on board a marine DP vessel. In Figure 2.9 these actuators are shown.

Figure 2.8: Offshore supply vessel [12].

- **Main propellers:** these actuators are mounted aft of the vessel's hull and produce forces parallel to the vessel's longitudinal axis.
- **Tunnel thrusters:** these actuators produce forces parallel to the vessel's transversal axis. They are mounted transverse through the hull of the vessel.
- **Azimuth thrusters:** these thrusters are mounted under the hull of the vessel and produce forces both in the longitudinal and transversal direction due to their rotational properties.

The commanded forces and moment $\tau \in \Re^3$ (surge, sway and yaw) can be written as follows according to [11]:

$$\tau = T(\alpha)Ku \tag{2.17}$$

where $f = Ku \in \Re^r$ (r is the number of actuators) is the thrust force vector and $u \in \Re^r$ is a DP control variable. K is a diagonal thrust coefficient matrix and $T(\alpha) \in \Re^{3\times r}$ is the actuator configuration matrix.

In this assignment only the forces in surge is of interest. This means that the tunnel thrusters are out of the question and that the azimuth thruster angle is zero. It is assumed that the surface vessel has two azimuth thrusters and two main propellers. The thrust coefficients for the azimuth thrusters are assumed to be $k_1 = k_2 = 137e^3$, and for the main propellers $k_3 = k_4 = 370e^3$. The DP control variable (u) can vary between ± 1.0. This result in a total surge force $\tau_{max} = 1014kN$, where the azimuth thrust force contribution is 27%. The coefficients and the control variable are based on the values found in the 'MatLab Marine GNC Toolbox' and on the values found in [11].

With a maximum force $\tau_{max} = 1014kN$ and with an operational speed of $u_v = 0.1m/s$, the total horizontal towing force $F_{t,x}max$ is:

$$F_{t,x}max = \tau_{max} - d_v u_v \approx 1009kN \tag{2.18}$$

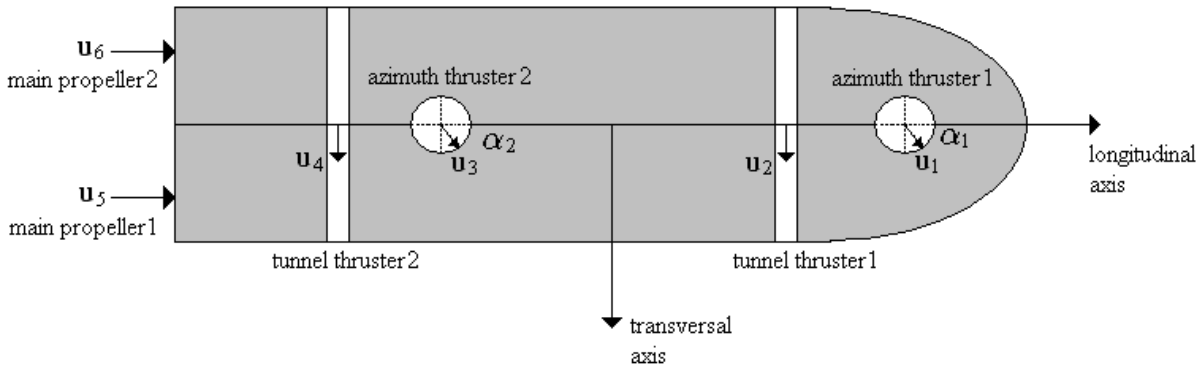

Figure 2.9: The most common actuators on board a marine DP vessel [11].

2.3 Mathematical Model of the Plough

2.3.1 Simplified Plough Model

From the assumptions in chapter 2.1.3 a simplified motion model for the plough can be derived. Two distinct orthogonal reference frames are employed in the derivation of the mathematical model, an inertial reference frame and a plough body-fixed reference frame. The inertial (global fixed) reference frame (X, Z) is defined with the origin located at the ocean surface where X is the horizontal direction defined positive to the north and Z is the vertical direction defined positive downwards, as shown in Figure 2.10. The plough body-fixed frame (X_{pb}, Z_{pb}) is fixed at the bottom of the plough share. X_{pb} is defined positive along the plough's longitudinal symmetry axis and Z_{pb} is defined positive upwards, see Figure 2.11.

The plough's equation of motion along the longitudinal axis is the significant motion component. The plough's equation of motion in the north direction can be described by Newton's Second Law as follows:

$$\begin{aligned} \dot{x}_p &= u_p \\ m_p \dot{u}_p &= F_{t,x} - d_p(u_p) \end{aligned} \tag{2.19}$$

where x_p is the plough's X position in the inertial reference frame, u_p denotes the plough's speed in surge (longitudinal speed), $\dot{u}_p$ denotes the plough's surge acceleration, m_p denotes the plough's mass and $F_{t,x}$ is the horizontal component of the towline force acting on the plough in the north direction. $d_p(u_p)$ is the plough's friction damping due to penetration of the seabed-sediment:

$$d_p(u_p) = f_p(u_p)u_p + b_p \tag{2.20}$$

where $f_p(u_p)$ is the speed-dependent part of the friction force and b_p is the static part of this force. These two parts are to be evaluated below.

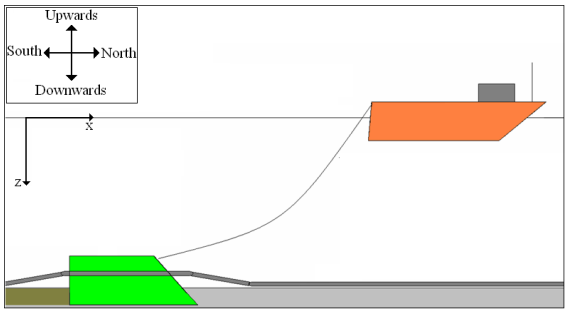

Figure 2.10: The plough's inertial reference frame (XZ-plane).

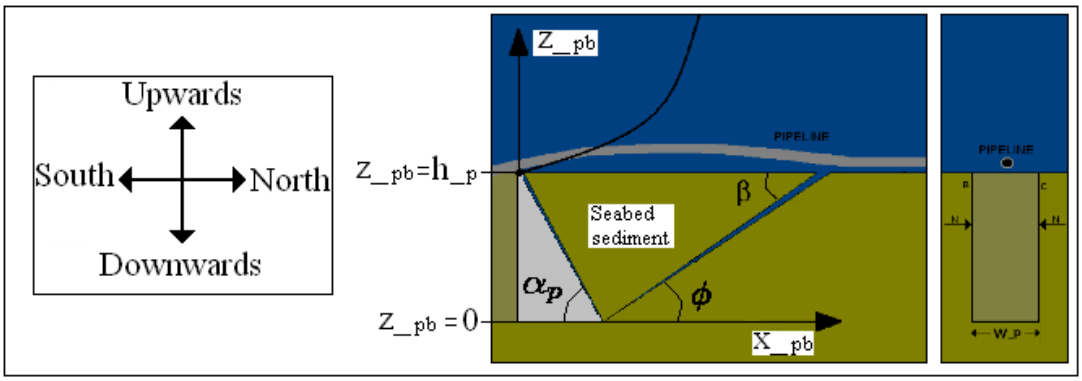

Figure 2.11: Plough share penetrating the seabed sediment.

2.3.2 Derivation of the Plough's Friction Force

Operations in thick seabed-sediment require large towing forces. This is partly, according to [5], due to the pore water effect. When compact seabed-sediment is pushed, the grains of sediment are rolled over one another. In so doing, the pores between the grains expand. When the pressure in these pores decreases, there will become a vacuum which fills water into the pores. The drag of this permeating water squeezes the grains together, increasing the force on the plough. As the ploughing speed increases or the deeper the burial, the greater the decrease in pore water pressure, and hence the greater the friction force. At some limiting ploughing speed either cavitation or grain crushing will occur. The cavitation limit is a function of ocean depth and the grain crushing limit is a function of the sediment properties.

The force induced when the plough penetrates the seabed-sediment mainly effects the plough's surge motion (motion along the plough's longitudinal axis). Reference [5] gives an analysis of the friction force on a finite-width plough share in dense ocean bottom sand. The size of the force acting on the plough from the seabed-sediment depends on the plough's speed in surge, ocean depth, burial depth and width (shape of the plough share) and various seabed-sediment parameters. The various parameters are the sediments friction angle (ϕ) formed by the plough share, the density (ρ_{ss}) of the seabed-sediment, the permeability (k) of the seabed-sediment, unconfined volumetric strain (ϵ_ν) and critical confining stress (σ_{crit}).

Based on Colomb's passive earth pressure theory, the force required to push a smooth vertical wall into cohesionless sediment is given by the following equation:

$$F_0 = \left(\frac{\rho_{ss} w_p h_p^2}{2} \right) \cdot N_\phi \tag{2.21}$$

where w_p and h_p are the width and height of the wall (ploug share), respectively, and N_ϕ is the ratio of the major and minor principle stress. N_ϕ is calculated as follows:

$$N_\phi = \left[tan \left(\frac{\pi}{4} + \frac{\phi}{2} \right) \right]^2 \tag{2.22}$$

where $\phi = \pi - \alpha_p - 2\beta$ is the friction angle of the seabed-sediment. ϕ, α_p and β are shown in Figure 2.11. Equation 2.21 gives results that are much smaller than those experienced in actual ocean ploughing. In actual ocean ploughing, the seabed-sediment force acting on the plough increases linearly with the ploughing speed. As the speed increases, a pore water effect causes the force to rise steeply up to some threshold, which is either the cavitation limit or the grain crushing limit.

Pore Water Effect

The pore water effect is a factor caused by the expansion of the sediment as it fails. Void volume is created by the sediment grains rolling over one another and has a generated

rate $u_p w_p h_p \epsilon_\nu$, where u_p is the plough's surge speed. When dividing this rate by the flow area one get the velocity of the created pore water flow as a function of z_{pb} (distance above the plough share bottom, see Figure 2.11):

$$V_{pore} = \frac{u_p \epsilon_\nu}{2} \cdot \left(\frac{z_{pb}}{h_p} \right) \tag{2.23}$$

The necessary pore water pressure gradient is as follows:

$$\frac{dP}{dz_{pb}} = \frac{\rho_{sw} V_{pore}}{k} = \frac{\rho_{sw} u_p \epsilon_\nu}{2k} \cdot \left(\frac{z_{pb}}{h_p} \right) \tag{2.24}$$

By integrating equation 2.24 one get the pressure profile:

$$\begin{aligned} \int dP &= \int \frac{\rho_{sw} u_p \epsilon_\nu}{2k} \cdot \left(\frac{z_{pb}}{h_p} \right) dz_{pb} \Rightarrow \\ P(z_{pb}) &= \frac{\rho_{sw} u_p \epsilon_\nu}{4k} \cdot \left(\frac{z_{pb}^2}{h_p} \right) + C \end{aligned} \tag{2.25}$$

By setting $z_{pb} = h_p$ the constant C is found:

$$\begin{aligned} P(z_{pb} = h_p) = (\rho_{sw} H_{sea} + P_{atm}) &= \frac{\rho_{sw} u_p \epsilon_\nu}{4k} \cdot \left(\frac{h_p^2}{h_p} \right) + C \quad \Rightarrow \\ C = (\rho_{sw} H_{sea} + P_{atm}) &- \frac{\rho_{sw} u_p \epsilon_\nu}{4k} \cdot \left(\frac{h_p^2}{h_p} \right) \quad \Rightarrow \\ P(z_{pb}) = (\rho_{sw} H_{sea} + P_{atm}) &- \frac{\rho_{sw} u_p \epsilon_\nu}{4k} \cdot \left(\frac{h_p^2 - z_{pb}^2}{h_p} \right) \end{aligned} \tag{2.26}$$

where H_{sea} is the ocean depth and P_{atm} is the atmospheric pressure. The pressure profile can be seen in Figure 2.12. In this figure it can be seen that the pressure decreases quadratically from the seabed surface to the plough share bottom. The profiles in this figure are based on the ploug's maximum operating depth $H_{sea,max} = 1000m$, the plough's height $h_p = 1.5m$, and different plough speed from $u_p = 0m/s$ to $u_p = 5m/s$. The plough speed is normally not as high as $5m/s$, but in this case it is just to get a large scope. This pressure appears as if the sediment's weight has increased. The effective seabed-sediment density becomes:

$$\begin{aligned} (\rho_{ss})_{eff} &= \rho_{ss} + \left(\frac{dP}{dz_{pb}} \right)_{avg} \quad \Rightarrow \\ (\rho_{ss})_{eff} &= \rho_{ss} + \frac{\rho_{sw} u_p \epsilon_\nu}{4k} \quad \Rightarrow \\ (\rho_{ss})_{eff} &= \rho_{ss} \left[1 + \frac{\rho_{sw}}{\rho_{ss}} \cdot \frac{u_p \epsilon_\nu}{4k} \right] \end{aligned} \tag{2.27}$$

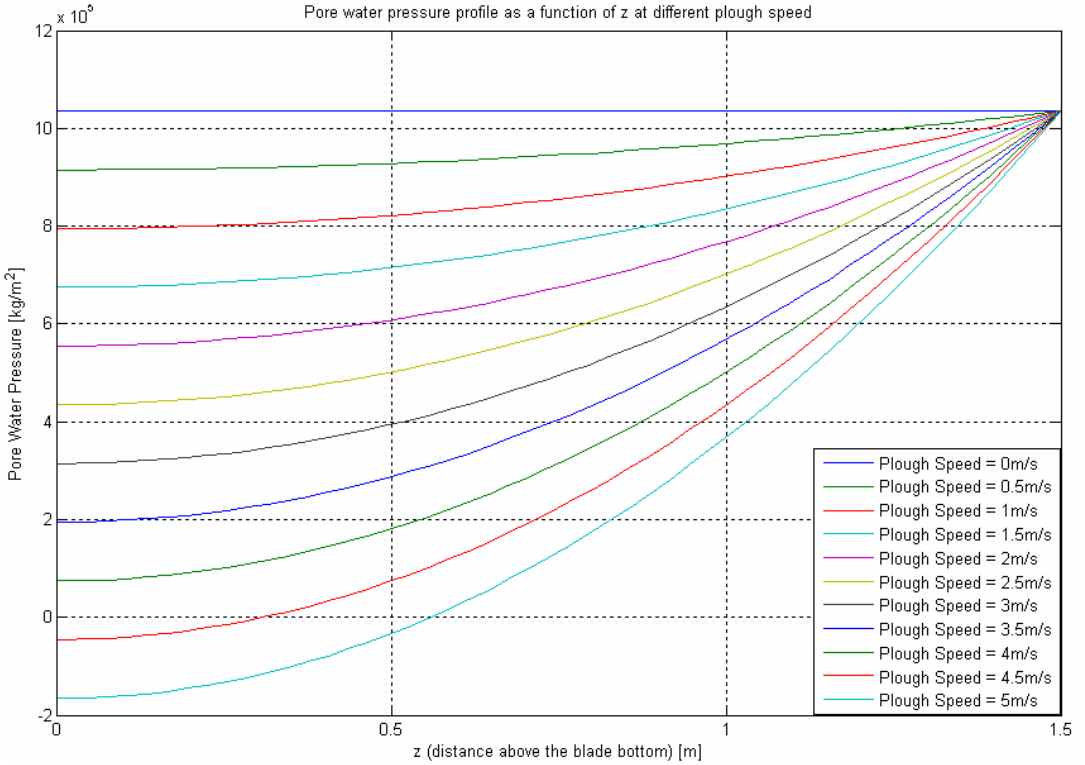

Figure 2.12: Pore water pressure profiles as a function of z_{pb} (distance above the plough share bottom) at different plough speed.

When substituting $(\rho_{ss})_{eff}$ into equation 2.21 the friction force, influenced by the pore water effect, is formulated as follows:

$$\begin{aligned} F_{0,pore} &= \left(\frac{\rho_{ss} w_p h_p^2}{2}\right) \cdot N_\phi \cdot \left[1 + \left(\frac{\rho_{sw}}{\rho_{ss}}\right) \cdot \left(\frac{u_p \epsilon_{\nu,0}}{4k}\right)\right] \Rightarrow \\ F_{0,pore} &= F_0 \cdot N_{pore} \end{aligned} \tag{2.28}$$

where $\epsilon_{\nu,0} = \epsilon_\nu$, F_0 is given by 2.21 and N_{pore} is the pore water factor:

$$N_{pore} = 1 + \left(\frac{\rho_{sw}}{\rho_{ss}}\right) \cdot \left(\frac{u_p \epsilon_{\nu,0}}{4k}\right) \tag{2.29}$$

Cavitation Limit

From Figure 2.12 and equation 2.26 one can see that the absolute seawater pressure at the plough share bottom ($z_{pb} = 0$) becomes smaller and smaller as the plough speed increases. The pressure eventually reaches the vapor pressure of the seawater. This is

the point where cavitaion begins. Further speed increase causes a cavitation region to grow in size and extend up the plough share. The effective sediment density over the uncavitated depth is, according to reference [5], as follows:

$$(\rho_{ss})_{eff} = \frac{dP}{dz_{pb}} = \left(\frac{\rho_{sw} H_{sea} + P_{atm}}{h_p - Z_c}\right) \tag{2.30}$$

where $z_{pb} = Z_c$ is the vertical extent of the cavitated region above the plough share bottom. When substituting $h_p - Z_c$ for h_p and $(\rho_{ss})_{eff}$ for ρ_{ss} in equation 2.21, the passive earth force on the plough share over the uncavitated depth is:

$$F_{cav,1} = \left(\frac{\rho_{sw} H_{sea} + P_{atm}}{h_p - Z_c}\right) \cdot \left(\frac{w_p (h_p - Z_c)^2}{2} \cdot N_\phi\right) \tag{2.31}$$

and over the cavitated depth Z_c the passive earth force on the plough share is:

$$F_{cav,2} = (\rho_{sw} H_{sea} + P_{atm}) \cdot (w_p Z_c N_\phi) \tag{2.32}$$

The total passive earth force on the plough share due to pore water permeation is the sum of equation 2.31 and 2.32:

$$\begin{aligned} &F_{cav,3} = F_{cav,1} + F_{cav,2} \Rightarrow \\ &F_{cav,3} = \left(\frac{\rho_{sw} H_{sea} + P_{atm}}{2}\right) \cdot (h_p + Z_c) \cdot w_p N_\phi \end{aligned} \tag{2.33}$$

To equation 2.33 one must add the small contribution due to the actual sediment weight. This gives:

$$F_{cav,4} = \left[\left(\frac{\rho_{sw} H_{sea} + P_{atm}}{2}\right) \cdot (h_p + Z_c) + \frac{\rho_{ss} h_p^2}{2}\right] \cdot w_p N_\phi \tag{2.34}$$

The friction force continues to increase after incipient cavitation until the cavitation region has grown to the seabed surface ($Z_c = h_p$). At this point the limiting force is reached and the friction force, influenced by cavitation, becomes as follow:

$$\begin{aligned} &F_{0,cav} = \left[(\rho_{sw} H_{sea} + P_{atm}) \cdot h_p + \frac{\rho_{ss} h_p^2}{2}\right] \cdot w_p N_\phi \Rightarrow \\ &F_{0,cav} = F_0 \cdot N_{cav} \end{aligned} \tag{2.35}$$

where N_{cav} is the cavitation factor:

$$N_{cav} = 1 + 2 \cdot \left(\frac{\rho_{sw}}{\rho_{ss}}\right) \cdot \left(\frac{H_{sea} + H_{atm}}{h_p}\right) \tag{2.36}$$

where $H_{atm} = \frac{P_{atm}}{\rho_{sw} g}$ is the atmospheric pressure expressed as height of seawater and g is the earth gravity constant.

Grain Crushing Limit

At large ocean depths, the sea pressure inhibits cavitation. When the ocean depth becomes large enough the sediment grains start crushing due to large contact pressure between them. The crushing pressure (average compressive stress) is given by:

$$\sigma_{avg} = \frac{\sigma_x + \sigma_y + \sigma_z}{3} \qquad \sigma_z < \sigma_y < \sigma_x \tag{2.37}$$

where σ_x is the sediment stress in the ploughing direction, σ_y is the sediment stress in the lateral direction and σ_z is the sediment stress in the vertical direction. When approximating the confining (bounded) stress ($\sigma_{conf} = \sigma_{avg}$), this can be done by taking an upper and lower bound of the lateral stress σ_y:

- For an upper bound when $\sigma_y = \sigma_x$:

$$(\sigma_{avg})_{upper} = \frac{2\sigma_x + \sigma_z}{3} \tag{2.38}$$

- For the lower bound when $\sigma_y = \sigma_z$:

$$(\sigma_{avg})_{lower} = \frac{\sigma_x + 2\sigma_z}{3} \tag{2.39}$$

According to the Mohr-Coulomb's failure criterion for cohesionless sediment, the ratio of the major principle stress (σ_x) to the minor principle stress (σ_z) is given by equation 2.22:

$$N_\phi = \left[tan\left(\frac{\pi}{4} + \frac{\phi}{2}\right)\right]^2 = \frac{\sigma_x}{\sigma_z} \tag{2.40}$$

The upper and lower bound for the ratio $\left(\frac{\sigma_z}{\sigma_{avg}}\right)$ can be found by substituting the expression for σ_x, in equation 2.40, into equation 2.38 and 2.39. The upper and lower bound for this ratio will get the following form:

- Upper bound:

$$\frac{\sigma_z}{(\sigma_{avg})_{upper}} = \frac{3}{2N_\phi + 1} \tag{2.41}$$

- Lower bound:

$$\frac{\sigma_z}{(\sigma_{avg})_{lower}} = \frac{3}{N_\phi + 2} \tag{2.42}$$

To get an overall estimate of σ_z, one can take the average of equation 2.41 and 2.42. This average is denoted as ψ_{ss}:

$$\begin{aligned} \psi_{ss} &= \left(\frac{\sigma_z}{\sigma_{avg}}\right)_{avg} \quad \Rightarrow \\ \psi_{ss} &= \frac{\frac{\sigma_z}{(\sigma_{avg})_{upper}} + \frac{\sigma_z}{(\sigma_{avg})_{lower}}}{2} \quad \Rightarrow \\ \psi_{ss} &= \frac{4.5(N_\phi + 1)}{(2N_\phi + 1) \cdot (N_\phi + 2)} \end{aligned} \tag{2.43}$$

The vertical sediment stress σ_z can be related to the confining stress ($\sigma_{conf} = \sigma_{avg}$):

$$\sigma_z = \psi_{ss} \cdot \sigma_{conf} \tag{2.44}$$

The relationship between confining stress and dilation can be formulated as follows:

$$\left(\frac{\sigma_{conf}}{\sigma_{crit}}\right)^2 + \left(\frac{\epsilon_\nu}{\epsilon_{\nu,0}}\right)^2 = 1 \tag{2.45}$$

where σ_{crit} is the critical confining stress, that appears when $\epsilon_\nu = 0$, and $\epsilon_{\nu,0}$ is the volumetric strain of dilating sediment for zero confining stress.

To get the final result for pore water effect, modified by grain crushing, one has to consider the vertical pressure profiles in Figure 2.12. The pressure decreases quadratically to the plough share bottom. Since the total stress at any given depth is constant the decrease in pore water pressure must be accompanied by an equal increase in the sediments vertical stress (σ_z). This gives raise to the following equation:

$$\begin{aligned} \Delta P = \sigma_z &= P(h_p) - P(0) \Rightarrow \\ \Delta P &= \frac{\rho_{sw} u_p h_p \epsilon_\nu}{4k} \end{aligned} \tag{2.46}$$

where ΔP is the pore water pressure decrease between the seabed and the plough share bottom. P is the pressure derived in equation 2.26. From equation 2.46 the volumetric strain can be formulated as follows:

$$\epsilon_\nu = \frac{4k\sigma_z}{\rho_{sw} u_p h_p} \tag{2.47}$$

By combining equation 2.44, 2.45 and 2.47 gives σ_z in terms of known parameters:

$$\sigma_z = \frac{1}{\sqrt{\left(\frac{1}{\psi_{ss}\sigma_{crit}}\right)^2 + \left(\frac{4k}{\rho_{sw} h_p u_p \epsilon_{\nu,0}}\right)^2}} \tag{2.48}$$

The effective increase in the sediment's density at the plough share bottom is:

$$(\rho_{ss})_{eff} = \rho_{ss} \cdot \left(1 + \frac{\sigma_z}{\rho_{ss} h_p}\right) \tag{2.49}$$

When substituting equation 2.49 for ρ_{ss} in equation 2.21 the friction force, influenced by grain crushing, becomes as follow:

$$F_{0,grc} = F_0 \cdot N_{grc} \tag{2.50}$$

where N_{grc} is the grain crushing factor which increases the friction force:

$$\begin{aligned} N_{grc} &= 1 + \frac{\sigma_z}{\rho_{ss} h_p} \Rightarrow \\ N_{grc} &= 1 + \frac{1}{\sqrt{\left(\frac{h_p \rho_{ss}}{\psi_{ss} \sigma_{crit}}\right)^2 + \left(\frac{4k\rho_{ss}}{\rho_{sw} u_p \epsilon_{\nu,0}}\right)^2}} \end{aligned} \tag{2.51}$$

2.3.3 Analysis of the Plough's Friction Force

While equation 2.21 gives the solution based on an infinitely-wide vertical plough share, the solution for a finite-width plough share, is according to [5], as follows:

$$d_p(u_p) = F_0 \cdot N_x \tag{2.52}$$

where F_0 is at all times replaced with the force factor $F_{0,pore}$ from equation 2.28, $F_{0,cav}$ from equation 2.35 or $F_{0,grc}$ from equation 2.50, whichever is smaller, and N_x is the finite-width factor:

$$N_x = \frac{\left(\frac{sin(\alpha_p)+\mu cos(\alpha_p)}{N_\phi}\right) \cdot \left(\frac{1}{tan(\alpha_p)} + tan\left(\frac{\phi}{2} + \frac{\alpha_p}{2}\right)\right) \cdot \left[\frac{N_\phi sin(\phi)}{3} \cdot \left(\frac{h_p}{w_p}\right) + cos\left(\frac{\phi}{2} - \frac{\alpha_p}{2}\right)\right]}{cos\left(\frac{\phi}{2} + \frac{\alpha_p}{2}\right) - \mu sin\left(\frac{\phi}{2} + \frac{\alpha_p}{2}\right)} \tag{2.53}$$

where α_p, h_p and w_p are the plough shares angle, height and width, respectively, as shown in Figure 2.5 in chapter 2.1.3. μ is the seabed-sediment on plough share friction coefficient and ϕ is the sediment's friction angle. For simplicity, only one of the force factors is wanted in the final friction force. A comparison between the three force factors has to be carried out in order to decide which factor to use.

Comparison Between $F_{0,pore}$ ***and*** $F_{0,grc}$

First a comparison between the speed dependent factors ($F_{0,pore}$ and $F_{0,grc}$) are carried out to prove that $F_{0,pore}$ is greater than or equal to $F_{0,grc}$. The parameter reduction

process is as follows:

$$\begin{aligned}
F_{0,pore} &\geq F_{0,grc} &&\Rightarrow \\
F_0 \cdot N_{pore} &\geq F_0 \cdot N_{grc} &&\Rightarrow \\
N_{pore} &\geq N_{grc} &&\Rightarrow \\
1 + \left(\frac{\rho_{sw}}{\rho_{ss}}\right) \cdot \left(\frac{u_p \epsilon_{\nu,0}}{4k}\right) &\geq 1 + \frac{1}{\sqrt{\left(\frac{h_p \rho_{ss}}{\psi_{ss} \sigma_{crit}}\right)^2 + \left(\frac{4k\rho_{ss}}{\rho_{sw} u_p \epsilon_{\nu,0}}\right)^2}} &&\Rightarrow \\
\left(\frac{\rho_{sw}}{\rho_{ss}}\right) \cdot \left(\frac{u_p \epsilon_{\nu,0}}{4k}\right) &\geq \frac{\rho_{sw} u_p \epsilon_{\nu,0}}{\left(\sqrt{\left(\frac{h_p \rho_{sw} u_p \epsilon_{\nu,0}}{4k\psi_{ss}\sigma_{crit}}\right)^2 + 1}\right) \cdot 4k\rho_{ss}} &&\Rightarrow \\
1 &\geq \frac{1}{\sqrt{\left(\frac{h_p \rho_{sw} u_p \epsilon_{\nu,0}}{4k\psi_{ss}\sigma_{crit}}\right)^2 + 1}}
\end{aligned} \tag{2.54}$$

From the comparison in 2.54 it can be seen that $F_{0,grc}$ is at all times less than or equal to $F_{0,pore}$ and that the two force factors are equal only when the ploughing speed is $0m/s$. The choice of force factor fall down to the grain crushing factor ($F_{0,grc}$).

Comparison Between $F_{0,grc}$ ***and*** $F_{0,cav}$

In this second comparison, between the plough speed dependent factor ($F_{0,grc}$) and the ocean depth dependent factor ($F_{0,grc}$), a case study has to be carried out to prove when $F_{0,grc}$ is less than or equal to $F_{0,cav}$. In this case study the plough and seabed-sediment data in Table 2.1 are used.

Let us first consider the grain crushing force factor ($F_{0,grc}$). When the plough speed $u_p \to \infty$ an upper limit value is found for $F_{0,grc}$. With the data from Table 2.1 this value becomes as follows:

$$\lim_{u_p \to \infty} (F_{0,grc}) = \lim_{u_p \to \infty} F_0 \cdot \left(1 + \frac{1}{\sqrt{\left(\frac{h_p \rho_{ss}}{\psi_{ss} \sigma_{crit}}\right)^2 + \left(\frac{4k\rho_{ss}}{\rho_{sw} u_p \epsilon_{\nu,0}}\right)^2}}\right) = \underline{F_0 \cdot 25.2} \tag{2.55}$$

When the plough speed $u_p \to 0$ a lower limit value is found for $F_{0,grc}$. With the data from Table 2.1 this value becomes as follows:

$$\lim_{u_p \to 0} (F_{0,grc}) = \lim_{u_p \to 0} F_0 \cdot \left(1 + \frac{1}{\sqrt{\left(\frac{h_p \rho_{ss}}{\psi_{ss} \sigma_{crit}}\right)^2 + \left(\frac{4k\rho_{ss}}{\rho_{sw} u_p \epsilon_{\nu,0}}\right)^2}}\right) = \underline{F_0} \tag{2.56}$$

In Figure 2.13 the grain crushing force factor ($F_{0,grc}$), divided by F_0, is shown as a function of the ploughing speed.

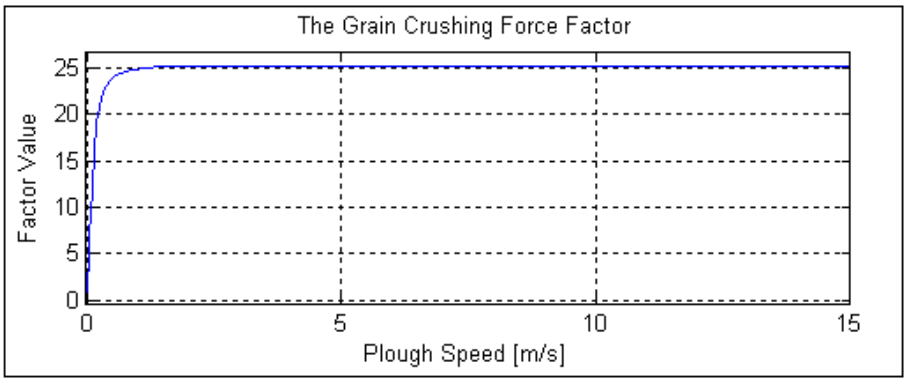

Figure 2.13: The grain crushing force factor, divided by F_0, as a function of the ploughing speed.

Plough and Sediment Data	Value
Plough width (w_p)	0.5m.
Plough height (h_p)	1.5m.
Plough speed (u_p)	$u_p \in [0, \infty]$.
Plough share angle (α_p)	30deg.
Seawater density (ρ_{sw})	$1025 \frac{kg}{m^3}$.
Earth gravity (g)	$9.81 \frac{m}{s^2}$.
Atmospheric pressure (P_{atm})	101325pa.
Seabed-sediment type	Nevada sand.
Permeability of sand (k)	$8.001 \cdot 10^{-5} \frac{m}{s}$.
Sands volumetric strain ($\epsilon_{v,0}$)	0.05.
Density of sand (ρ_{ss})	$1087.8 \frac{kg}{m^3}$.
Sands critical confining stress (σ_{crit})	$98429.7 \frac{kg}{m^2}$.
Sands friction angle (ϕ)	38deg.
Sand on plough share friction coefficient (μ)	0.
Ocean depth (H_{sea})	Grain crushing limit.

Table 2.1: Plough and sediment data used in the case study when comparing $F_{0,grc}$ with $F_{0,cav}$.

Let us now consider the cavitation force factor ($F_{0,cav}$). What is of interest here is to find the ocean depth where the grain crushing limit is reached. This is the upper limit for the grain crushing force factor ($\lim_{upper}(F_{0,grc}) = F_0 \cdot 25.2$). With the data from Table 2.1, the ocean depth is found as follows:

$$\begin{aligned} F_{0,cav} &= \lim_{upper}(F_{0,grc}) \quad \Rightarrow \\ F_0 \cdot N_{cav} &= F_0 \cdot 25.2 \quad \Rightarrow \\ 1 + 2 \cdot \left(\frac{\rho_{sw}}{\rho_{ss}}\right) \cdot \left(\frac{H_{sea} + H_{atm}}{h_p}\right) &= 25.2 \quad \Rightarrow \\ H_{sea} &\approx \underline{9.2m} \end{aligned} \tag{2.57}$$

In 2.57 the ocean depth (H_{sea}) is found to be $9.2m$. This is the depth where the cavitation force factor ($F_{0,cav}$) is equal to the grain crushing force factor ($F_{0,grc}$). At ocean depths below this depth, the cavitation force factor will exceed the grain crushing force factor.

2.3.4 Resulting Friction Force and Discussion

In this assignment, as was assumed in chapter 2.1.3, we are interested in ploughing operations on ocean depths far below $10m$. The grain crushing force factor ($F_{0,grc}$) is always smaller than the cavitation force factor at depths below $10m$, and at all times smaller than the pore water force factor. According to [5], $F_{0,grc}$ is the right choice and will replace F_0 in equation 2.52. The plough's final friction force can be formulated as follows:

$$\begin{aligned} d_p(u_p) &= F_{0,grc} \cdot N_x \Rightarrow \\ d_p(u_p) &= F_0 \cdot N_x \cdot \left(1 + \frac{u_p}{\sqrt{A^2 \cdot u_p^2 + B^2}}\right) \end{aligned} \tag{2.58}$$

where $A = \frac{h_p \rho_{ss}}{\psi_{ss} \sigma_{crit}}$ and $B = \frac{4k\rho_{ss}}{\rho_{sw} \epsilon_{\nu,0}}$. Equation 2.58 can be split up into the two parts formulated in equation 2.20 as follows:

$$f_p(u_p) = \frac{F_0 \cdot N_x}{\sqrt{A^2 \cdot u_p^2 + B^2}} \tag{2.59}$$

$$b_p = F_0 \cdot N_x \tag{2.60}$$

where $f_p(u_p)$ is the plough speed-dependent friction force and b_p is the static force due to the constant pressure on the plough share. The plough's final friction force profile in equation 2.58, when using the data from Table 2.1, is shown in Figure 2.14. In this figure it can be seen that the friction force is about $3.2mton$ at zero speed (static friction force b_p) and $56.6mton$ when the speed is $0.16m/s$. This is the assumed maximal operation speed. All ocean depths below $10m$ will give the same profile.

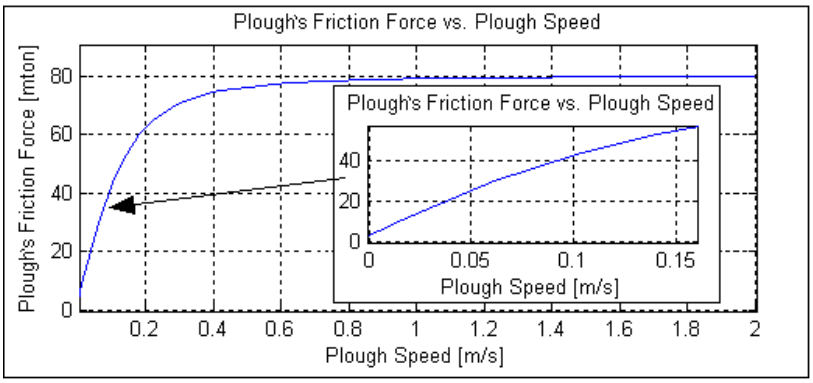

Figure 2.14: The plough's final friction force profile in metric tons.

Equation 2.58 is dependent on the ploughing speed (u_p) and it is nonlinear with a profile shaped as a sigmoid function. It is measured in metric tons and must be multiplied by the earth gravity constant (g) to be measured in Newton. The sediment data in Table 2.1 were found in reference [5], and are based on data from Nevada sand. The type of sediment on the ocean bottom is normally examined before the ploughing operation is begun. This examination is performed by a seismic vessel doing a seismic survey on the ocean bottom. The different type of sediment has different parameter values. For simplicity in this assignment, only the density of the sediment is changed when simulating a change of sediment type. The plough's equation of motion and its friction force is programmed into Simulink. This Simulink program is located on the appended CD found in appendix A under the folder "Plough AndSediment Model Sim".

2.4 Mathematical Model of the Towline

In the offshore industry, towline cables (fiber-ropes, steel-wires, chains, etc.) are used in many different applications. They are used by surface vessels for towing other surface vessels, underwater vehicles, platforms and other offshore installations. They are used in Position Mooring (PM) systems for surface vessels and platforms. They are also used in crane operations.

For over forty years, a lot of research effort has been devoted to the dynamics of marine cables. Despite the variety of the applications, their basic approaches are similarly based on the finite element method (FEM). The FEM-method is one of the most common methods used in industrial applications. Several software programs, based on the FEM-method, exist for analysis of submerged cables. These are:

- RIFLEX
- ABAQUS
- ANSYS

The software programs listed above make use of high fidelity models and are therefore not suited for control system design. They are also usually slower than software programs for a given application, see reference [1]. In this assignment we are interested in a low fidelity model which captures the main dynamics and which is easy to compute.

Previous Work by Others
Several papers have been written where the lumped mass method or the finite element method has been used to describe the towline's motion. In [1], a new finite element model of a submerged cable is derived for a moored operation. The hydrodynamic loads on the cable were modeled according to Morison's equation, and were assumed to dominate internal damping. Bending and torsion stiffness were assumed to be negligible to avoid increased implementation complexity and computation time. To avoid the numerical singularity that occurs for zero tension, assumptions are made for the mooring cables to be pretensioned. Global existence and uniqueness of solutions of the truncated system was shown. A simple test of the finite-element model was performed by comparing the static solution with the exact solution of the elastic Catenary equation. It was shown that the finite element method converged to the exact solution as the number of elements was increased.

Reference [23] gives an analysis of a control system structure of towed underwater vehicles (TUVs). A TUV has no thrusters and is towed by a surface vessel. The towline is modeled by a finite number of rigid elements. The elements have their masses lumped on the respective ends and connected by frictionless joints. The forces relative to each towline element are assumed to be applied to its point of mass. For modeling the equation of motion, the Lagrange method was used instead of the Newton-Euler method.

This was done to avoid redundant state-variable and constraint forces in the resulting model. The system analysis in [23] relies on a numerical method and hence it requires the specific values of the physical parameters involved. The system was shown to be mathematically controllable and observable.

Reference [21] is similar to [23]. A towed underwater vehicle is to keep a desired distance from the ocean bottom. The towline used was divided into several elements and modeled in two dimensions. The mass of each cable elements are lumped at the end of each element. A nonlinear adaptive Lyapunov-based controller was designed and tested in simulation. The results showed that this controller was adequate for bottom following applications and gave precise control of the attitude of a towed vehicle. The controller gave robust results in spite of uncertain vehicle parameter and bounded external disturbances. The lumped mass model is also used in reference [19] and [8].

2.4.1 Lumped Mass Method

Lumped mass means that the towline is divided into n elements and $n+1$ nodes. The mass of these elements are located in the nodes. The mass of one node equals the density of the towline multiplied with the volume of the element. The internal dynamic of towline element i is described by a spring tension (T_i) and an internal damping tension (P_i), see Figure 2.16. Two distinct orthogonal reference frames are employed in the development of the mathematical model, an inertial reference frame and a towline body-fixed reference frame. The inertial (global fixed) reference frame (X, Z) is defined with the origin located at the ocean surface where X is the horizontal direction defined positive to the north and Z is the vertical direction defined positive downwards, as shown in Figure 2.16. The body-fixed frame of element i $(X_{tb,i}, Z_{tb,i})$, is defined relative to the towline element, where $Z_{tb,i}$ is the direction normal to the towline element and $X_{tb,i}$ is the direction tangent to it. The position and orientation of each towline element is described with respect to the inertial reference frame, by two displacements, $x_{t,i}$ and $z_{t,i}$, and a single orientation angle θ_i as shown in Figure 2.15. The angle θ_i is defined positive clockwise.
In Figure 2.16, node n is located in the plough's center of gravity (CG) and node 0 is located in the surface vessel's CG. The acceleration of node 0 equals the acceleration of the surface vessel:

$$\ddot{x}_{t,0} = \dot{u}_{sv}, \qquad \ddot{z}_{t,0} = \dot{\omega}_{sv} \tag{2.61}$$

where $\ddot{x}_{t,0}$ and $\ddot{z}_{t,0}$ are the the horizontal and vertical acceleration of the towline's first node ($node0$) and $\dot{u}_{sv}$ and $\dot{\omega}_{sv}$ are the horizontal (x-direction) and vertical (z-direction) acceleration of the surface vessel. The equation of motion for node n can be written as follows:

$$m_e\ddot{x}_{t,n} = T_{x,n} + P_{x,n} - Fp_x + \frac{1}{2}D_{x,n} \tag{2.62}$$

$$m_e\ddot{z}_{t,n} = T_{z,n} + P_{z,n} + m_e g - B_e + Fp_z + \frac{1}{2}D_{z,n} \tag{2.63}$$

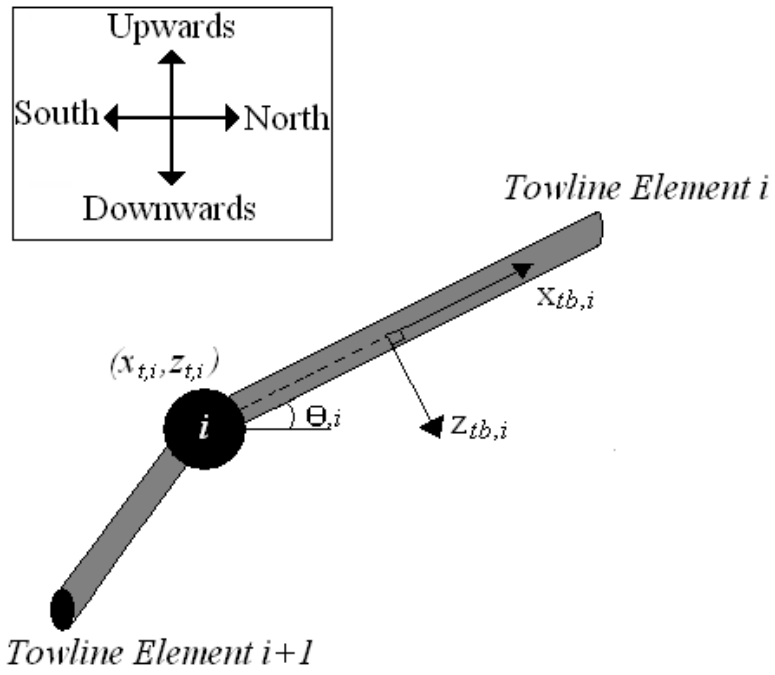

Figure 2.15: The towline-elements body fixed reference frame.

where $T_{x,n}$ and $T_{z,n}$ are the tension in each direction due to stiffness in element n, $P_{x,n}$ and $P_{z,n}$ are the towline's internal linear damping in each direction due to internal friction in element n and $D_{x,n}$ and $D_{z,n}$ are the hydrodynamic force on element n in each direction caused by drag. The direction sign of these forces are determined by the towline elements angle. $\ddot{x}_{t,n}$ and $\ddot{z}_{t,n}$ are the horizontal and vertical acceleration of node n, m_e is the mass of each towline element, B_e is the buoyancy force and g is the gravity force on each towline element, Fp_x is the horizontal force acting on the plough from the seabed sediment and Fp_z is the plough's vertical force due to gravitation and buoyancy. The equation of motion for node i, where $i \in [1, n-1]$, can be written as follows:

$$m_e\ddot{x}_{t,i} = T_{x,i} - T_{x,i+1} + P_{x,i} - P_{x,i+1} + \frac{1}{2}(D_{x,i} + D_{x,i+1}) \quad (2.64)$$

$$m_e\ddot{z}_{t,i} = T_{z,i} - T_{z,i+1} + P_{z,i} - P_{z,i+1} + m_e g - B_e + \frac{1}{2}(D_{z,i} + D_{z,i+1}) \quad (2.65)$$

Internal Forces

The internal dynamics of a towline can be described by a spring and damper system. The horizontal and vertical spring force in towline element i, where $i \in [1, n]$, can be written as follows according to Hook's law:

$$T_{x,i} = K_e(x_{t,i-1} - x_{t,i}) - K_e L_e \cos\theta_i, \quad \forall(x_{t,i-1} - x_{t,i}) \geq L_e \cos\theta_i \quad (2.66)$$

$$T_{z,i} = K_e(z_{t,i-1} - z_{t,i}) - K_e L_e \sin\theta_i, \quad \forall(z_{t,i} - z_{t,i-1}) \geq L_e \sin\theta_i \quad (2.67)$$

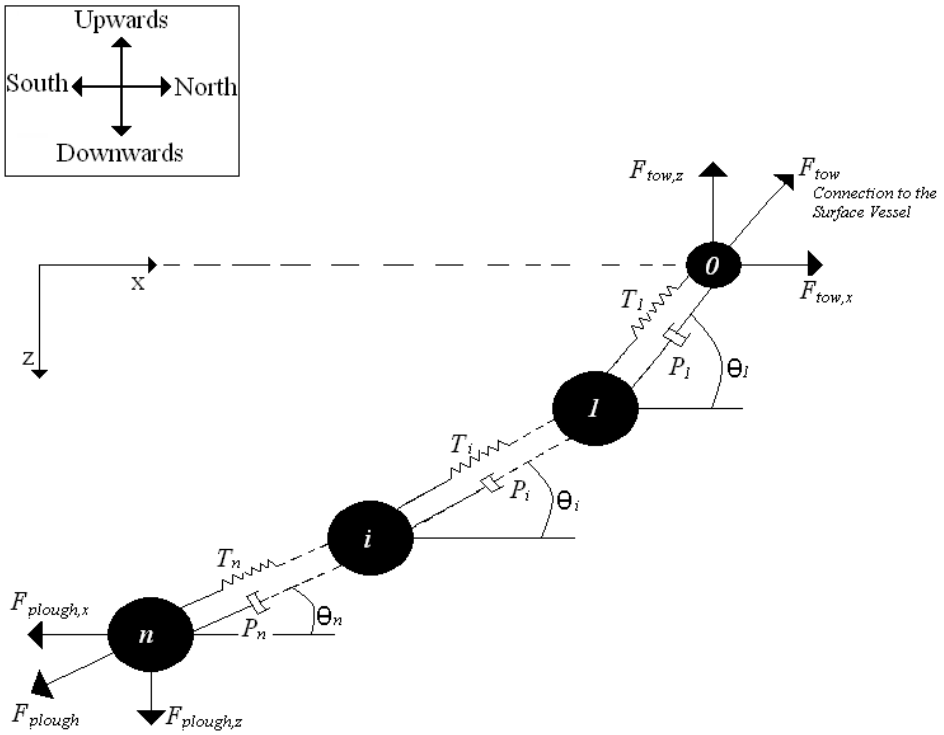

Figure 2.16: Principle sketch of the Lumped Mass Method (xz-plane).

where $x_{t,i}$ and $z_{t,i}$ are the position of element i in each direction in the inertial reference frame, L_e is the unstretched element length, θ_i is the angle between the inertial reference frame (X,Z) and body-fixed frame of element i. K_e is the spring constant:

$$K_e = \frac{EA_e}{L_e} \tag{2.68}$$

where E is Young's modulus for the towline and A_e is the towline's cross-section. The angle θ_i is calculated as follows:

$$\theta_i = \begin{cases} -\pi + \arctan\left(\frac{z_{t,i-1}-z_{t,i}}{x_{t,i-1}-x_{t,i}}\right), & \text{if } (x_{t,i-1}-x_{t,i}) < 0 \text{ and } (z_{t,i-1}-z_{t,i}) < 0 \\ \pi + \arctan\left(\frac{z_{t,i-1}-z_{t,i}}{x_{t,i-1}-x_{t,i}}\right), & \text{if } (x_{t,i-1}-x_{t,i}) < 0 \text{ and } (z_{t,i-1}-z_{t,i}) > 0 \\ \arctan\left(\frac{z_{t,i-1}-z_{t,i}}{x_{t,i-1}-x_{t,i}}\right), & \text{else} \end{cases} \tag{2.69}$$

The linear internal damping in the towline is created by friction between the braids in the towline. The tangential damping force is written as follows:

$$P_i = C_\nu(u_{t,i-1} - u_{t,i}) \tag{2.70}$$

where C_ν is the damping coefficient, $u_{t,i}$ is the longitudinal (tangential) speed of towline element i and $i \in [1, n]$. $u_{t,i-1} - u_{t,i}$ is calculated as follows:

$$u_{t,i-1} - u_{t,i} = (\dot{x}_{t,i-1} - \dot{x}_{t,i}) \cdot \cos\theta_i + (\dot{z}_{t,i-1} - \dot{z}_{t,i}) \sin\theta_i \tag{2.71}$$

By combining equation 2.70 and 2.71 the internal damping force can be divided into a horizontal and vertical component in the following way:

$$P_{x,i} = C_\nu(\dot{x}_{t,i-1} - \dot{x}_{t,i}) \tag{2.72}$$

$$P_{z,i} = C_\nu(\dot{z}_{t,i-1} - \dot{z}_{t,i}) \tag{2.73}$$

where $\dot{x}_{t,i}$ and $\dot{z}_{t,i}$ are respectively the horizontal and vertical speeds of element i.

External Forces

External forces on the towline are caused by the environment. Environmental forces are hydrodynamic drag and gravity. The tangential and normal components $(X_{tb,i}, Z_{tb,i})$ of the drag force, applied to towline element i, are found in reference [24] and can be written as follows:

$$D_{X_{tb,i}} = \frac{1}{2}\rho_{sw} C_{t,i} d |V_{t,i}| V_{t,i} \tag{2.74}$$

$$D_{Z_{tb,i}} = \frac{1}{2}\rho_{sw} C_{n,i} d |V_{n,i}| V_{n,i} \tag{2.75}$$

where $D_{X_{tb,i}}$ and $D_{Z_{tb,i}}$ are respectively the tangential and normal hydrodynamic drag force components on element i (per unit length of the towline), ρ_{sw} is the density of seawater and d is the diameter of the towline. $V_{t,i}$ and $V_{n,i}$ are respectively the tangential

and normal components of the seawater's relative speed over element i. $C_{t,i}$ and $C_{n,i}$ are respectively the tangential and normal drag coefficients that are dependent on the Reynolds number for the seawater speed relative to the towline element. The drag coefficients are usually determined experimentally and in reference [24] the following reported values are given for $C_{t,i}$ and $C_{n,i}$:

$$C_{t,i} = \begin{cases} 1.88/(R_{et})^{0.74}, & \text{for } 0.1 \leq R_{et} \leq 100.55 \\ 0.062, & \text{for } 100.55 \leq R_{et} \end{cases} \tag{2.76}$$

$$C_{n,i} = \begin{cases} 0.0, & \text{for } R_{en} \leq 0.1 \\ 0.45 + 5.93/(R_{en})^{0.33}, & \text{for } 0.1 \leq R_{en} \leq 400 \\ 1.27, & \text{for } 400 \leq R_{en} \leq 10^5 \\ 0.3, & \text{for } 10^5 \leq R_{en} \end{cases} \tag{2.77}$$

where the Reynolds numbers R_{et} and R_{en} are defined as

$$R_{et} = \rho_t d|V_{t,i}|/\mu_{sw}, \qquad R_{en} = R_{et} = \rho_t d|V_{n,i}|/\mu_{sw} \tag{2.78}$$

where ρ_t is the towline's density and μ_{sw} is the viscosity of seawater.

The relative speed of the seawater flow over a particular towline element is a function of the water speed and the element's velocity. The tangential and normal velocity components can be derived by using Figure 2.15 and are determined as follows:

$$V_{t,i} = (U_{x,i} - \dot{x}_i) \cdot \cos\theta_i + (U_{z,i} - \dot{z}_i) \cdot \sin\theta_i \tag{2.79}$$

$$V_{n,i} = (U_{x,i} - \dot{x}_i) \cdot \sin\theta_i + (U_{z,i} - \dot{z}_i) \cdot \cos\theta_i \tag{2.80}$$

where $U_{x,i}$ and $U_{z,i}$ are respectively the horizontal and vertical water flow velocities and $\theta_i \in [-180, 180]$. The horizontal and vertical components of the drag force, applied to element i, can be written as follows:

$$D_{x,i} = D_{Z_{tb,i}} L_e \sin\theta_i + D_{X_{tb,i}} L_e \cos\theta_i \tag{2.81}$$

$$D_{z,i} = D_{Z_{tb,i}} L_e \cos\theta_i + D_{X_{tb,i}} L_e \sin\theta_i \tag{2.82}$$

According to reference [14], one can assume that the water flow speed profile is horizontal. Usually the speed is smaller near the ocean bottom, and for simulation one can assume that the speed is constant from the water surface to a predefined ocean depth. The speed can then be reduced to a smaller constant value and change direction. The new value of the speed is then kept all the way to the ocean bottom. The reason for this change in water flow can e.g be because saltwater traveling from the south to the north will meet fresh water. The fresh water will then sink to a level near the ocean bottom and travel south, see Figure 2.17. By assuming that the water flow profile is as shown in Figure 2.17, the following can be stated:

$$\begin{array}{ll} U_{x,i} \geq 0, & \text{for } 0 \leq z_i < H_{fw} \\ U_{x,i} < 0, & \text{for } H_{fw} \leq z_i \leq H_{sea} \\ U_{z,i} = 0, & \text{for } z_i \in [0, H_{sea}] \end{array} \tag{2.83}$$

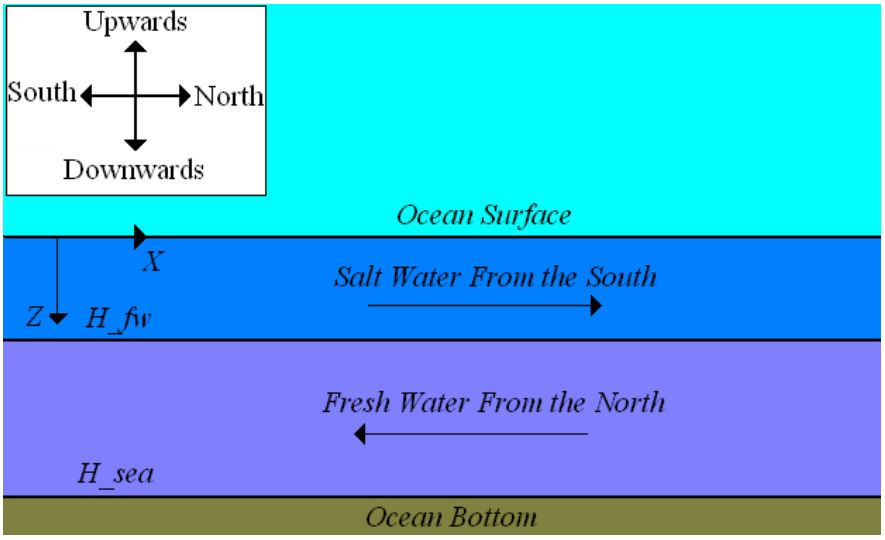

Figure 2.17: The water flow profile seen in the inertial reference frame.

where $z = H_{fw}$ is the ocean depth where the water flow changes and $z = H_{sea}$ is the depth from the ocean surface to the ocean bottom.

The mass (in kilogram) and gravity force of the cable elements are given by:

$$m_e = \rho_t \upsilon_e, \qquad B_e = \rho_{sw} \upsilon_e g \tag{2.84}$$

where ρ_t is the towline density, υ_e is the volume of the towline element and g is the acceleration due to gravity.

2.4.2 Choice of Towline

Before simulating the towline model, an appropriate type of towline with accompanying data must be found. According to [17], towlines made of fiber-rope are not proper for ploughing operations in shallow water. This is because the fiber is non resistant to seabed dust. For ploughing in deep water it is often that a combination of fiber-rope and steel-wire is used to reduce the weight of the towline. The fiber-rope is then attached to the surface vessel while the steel-wire is attached to the plough. Fiber-ropes are lightweight and more elastic compared to steel wires and are also suitable for lowering objects vertical into deep oceans. For simplicity in this assignment a pure steel-wire will be used.

The dimension of the towline and stiffness must be chosen according to the minimum breaking load (BL) for the vessel's towing winch and according to the vessel's towing capability. It is necessary that the towline breaks before the winch to avoid damage on human beings working on the vessel's deck. From chapter 2.2.2 it was derived that the

total horizontal towing force for the vessel was about $1009kN$, which is about $103mton$. It is therefore assumed that the safe working load (SWL) for the vessel's towing winch is $100mton$. From Figure 2.14 in chapter 2.3.2 it can be seen that the friction force on the plough (the horizontal pulling load) reaches approximately $60mton$ when it penetrates Nevada sand with a speed of $0.16m/s$ (assumed maximum operational speed). It is therefore necessary to choose a towline with larger horizontal SWL than $60mton$. The horizontal SWL for the towline is set to $SWL_x = 100mton$. Different safety factors (SF) are used depending on the damage the towline can do when it breaks. This factor can be in the range from $SF = 2$ to $SF = 10$. According to [13], the safety factor for a towline, used in ploughing operation, can be between 2.5 and 3. In this assignment a factor $SF = 2.5$ is chosen. This means that the minimum horizontal breaking load for the towline must be $BL_x = SWF_x \cdot SF = 250mton$.

It is necessary that the plough is kept at a constant depth. If the plough's depth changes due to large vertical towline tension, large damages to the pipeline (which the plough is to bury) might occur. This means that the weight of the plough must exceed or be equal to the vertical tension from the last towline element. When operating near the horizontal breaking load area, the angle (θ_n) between the plough's horizontal plane and the towline's last element must not exceed the following value:

$$\begin{aligned} \sum F_{plough,z} &\geq 0 \Rightarrow \\ m_p - BL_x \tan\theta_n &\geq 0 \Rightarrow \\ \theta_n &\leq \arctan\left(\frac{m_p}{BL_x}\right) \Rightarrow \\ \theta_n &\leq \arctan\left(\frac{52000}{250000}\right) \Rightarrow \\ \theta_n &\leq 11.7degree \end{aligned} \tag{2.85}$$

where BL_x is the minimum horizontal breaking load for the towline, m_p is the submerged weight of the plough and g is the earth gravity. By using the angle in 2.85, the tangential breaking load (BL) for the towline can be found as follows:

$$BL = \frac{BL_x}{\cos\theta_n} \approx 255.35mton \tag{2.86}$$

The minimum breaking load in equation 2.86 can be used when selecting a proper towline. In reference [2] a towline is chosen according to the minimum breaking load in equation 2.86, and the data is shown in Table 2.2.

The mass (m_e) and volume (υ_e) of one element, in equation 2.84, is calculated as follows:

$$m_e = (m_t/unitlength) \cdot L_e \tag{2.87}$$

$$\upsilon_e = A_e \cdot L_e \tag{2.88}$$

where $m_t/unitlength$ is the towline's mass (in kilogram) pr. meter, see Table 2.2.

Towline data	Value
Type	Steel wire rope.
Classification	6×19-IWRC.
Youngs Modulus (E)	$1.96 \cdot 10^9 N/m^2$.
Minimum breaking load in mton (BL)	$237mton$.
Diameter (d)	$0.057m$.
Weight ($m_t/unitlength$)	$13.9kg/m$.
Area (A_e)	$1.48 \cdot 10^{-3} m^2$.

Table 2.2: Towline Cable Data.

2.4.3 Analysis of The Towline Model

The model derived above is nonlinear due to quadratic hydrodynamic damping of the towline. The internal linear damping in the towline decides the elasticity amplitude in each towline element while the spring constant decides the elasticity frequency.

The internal damping coefficient in a towline is, according to [18], hard to find and can be disregarded when the towline is moving in seawater. This is due to hydrodynamic damping tangent to the towline. The internal damping can differ from one towline to another, and in order to find the coefficient, empirical experiments have to be made. In this assignment an experiment has not been available for the chosen towline described in Table 2.2.

A case study is performed where the towline is lowered vertically into the ocean. The towline is fastened to the vessel, which is kept steady. At the bottom end of the towline a mass of $1000kg$ is added. The towline's bottom end is given an impulse motion in the vertical direction. The elongation of the towline is measured without damping, with internal damping, with external quadratic damping and with both internal damping and external quadratic damping. In this case study the towline data from Table 2.2 was used. The length of the towline was set to $L = 348m$, the internal damping coefficient was chosen to a random number $C_\nu = 8980$ and the viscosity of seawater is $\mu_{sw} = 0.0012kg/(ms)$. In Figure 2.18 the results are shown. From this figure it can be seen that the initial elongation of the towline is about $3.75m$ and that the maximum amplitude, when exposed to an impulse motion is about $2m$. It can also be seen that the external quadratic damping caused by tangential drag has the same function as the internal towline damping, but with a larger amplitude. Of course this depends on the size of the internal damping coefficient. According to [14], it is often usual to add an external linear damping part to the towline's equation of motion for additional damping to get a better fit with the real world. This can only mean that the internal damping coefficient chosen for this case study must be in the right area.

When taking a closer look at Figure 2.18 it can be seen that the damped frequency of the towline is almost the same with different damping. The damped frequency can be

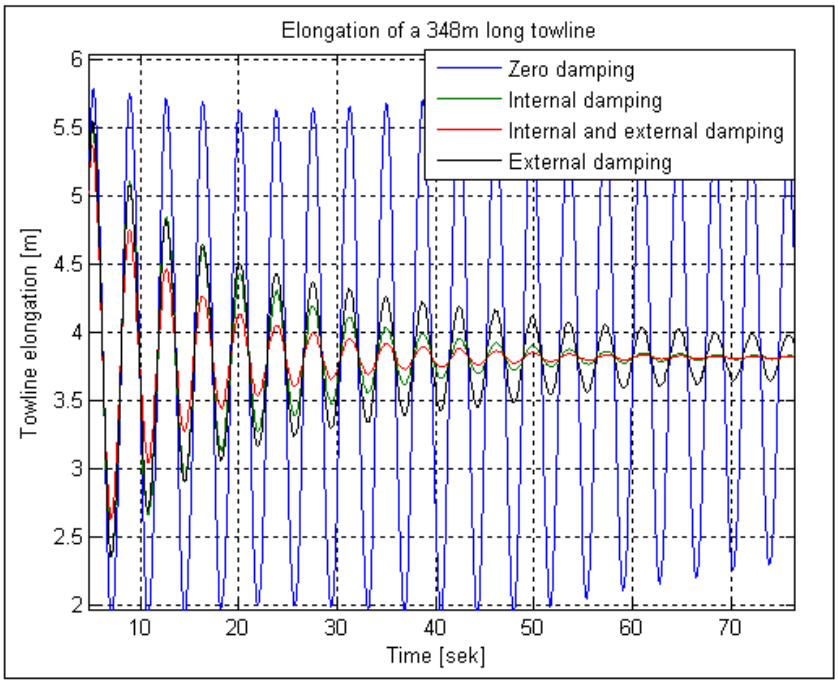

Figure 2.18: Elongation of the towline with different damping factors.

found from the figure (red curve: with external and internal damping), by counting the number of periods over a certain amount of time. The frequency was found to be about $f_t = 0.26Hz$. Converting to radians pr. second the frequency is $\omega_t = 2\pi f_t = 1.634rad/s$.

Another case study is performed to see how the hydrodynamic drag effects the towline's motion in the XZ-plane. The towline is lowered into the ocean like in the case study above with a mass of $1000kg$ added to the bottom end of the towline. But in this case the towline is given an angle relative to the vertical Z-plane. The towline is tied to the surface vessel with the position $(x_{t,0} = 285m, z_{t,0} = 0m)$ in the XZ-plane. The same towline data is used as before. The towline is released from its initial position and the motion in the XZ-plane is measured. The first measurement is done without hydrodynamic drag. The results are shown in Figure 2.19. It can be seen that the towline swings like a pendulum with very little damping. When the towline is exposed to hydrodynamic drag, the towline behaves like in Figure 2.20. From this figure it can be seen that the towlines motion is overdamped or critically damped. This is, according to [14], a realistic behavior for a towline moving in seawater.

2.4.4 Initializing the Towline Elements

Before the simulation of the ploughing operation can begin, the towline elements position has to be initialized. This is to avoid large transient motion in the beginning of the

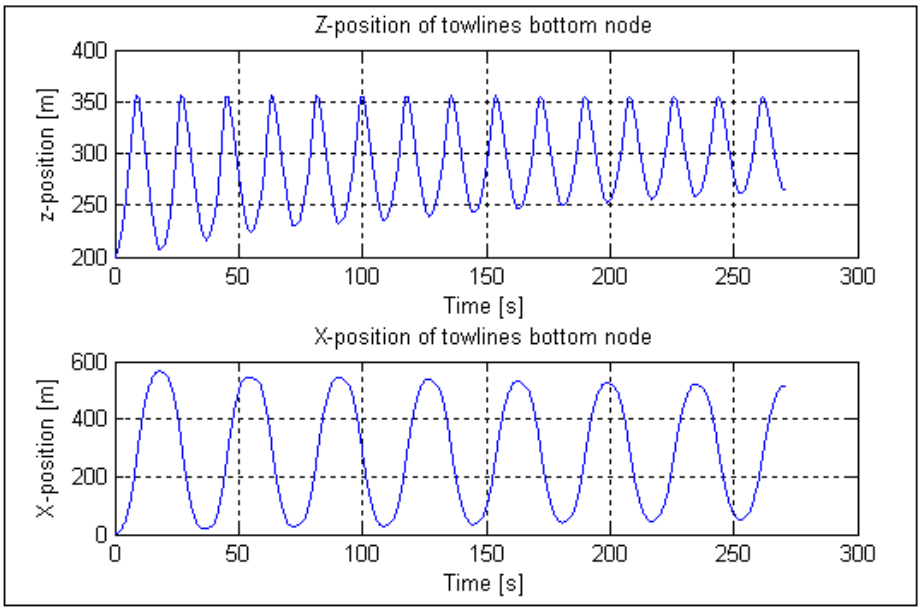

Figure 2.19: XZ-position of the bottom node when the towline swings like a pendulum and the top node has the location ($x_{t,0} = 285m, z_{t,0} = 0m$), (without drag forces).

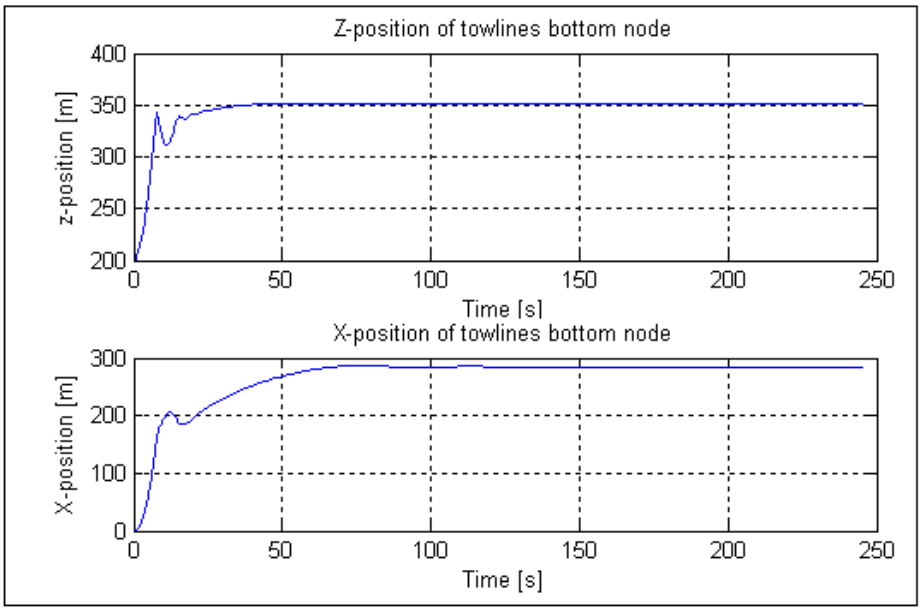

Figure 2.20: XZ-position of the bottom node when the towline swings like a pendulum and the top node has the location ($x_{t,0} = 285m, z_{t,0} = 0m$), (with drag forces).

simulation. When initializing the towline the two end nodes must be at rest. An experimental procedure can be carried out in order to initialize the towline as described below.

The Catenary curve

It is known that when a chain or rope is loosely hung between two fixed points, it hangs in a curve called a Catenary, which is a word derived from the Latin catena and means chain. This curve looks much like a parabola but it is not. The Catenary curve is shown in Figure 2.21 and the catenary equation can be formulated as follows to fit into the inertial reference frame:

$$z(x) = -a\left(\cosh\left(\frac{x}{a}\right) - 1\right) + H_{sea} \tag{2.89}$$

where H_{sea} is the ocean depth and a is a constant expressed in meters:

$$a = \frac{T_0}{m_t/unitlength} \tag{2.90}$$

where T_0 is the plough's horizontal static friction force ($F_0 \cdot N_x$), from equation 2.60 in subsection 2.3.4, and $m_t/unitlength$ is the towlines mass per unit length. According to [4] and many other calculus books, the total length of the Catenary curve can be found as follows:

$$s = \int_{x_0}^{x_n} \sqrt{1 + \left(\frac{dz}{dx}\right)^2}\, dx \tag{2.91}$$

where x_n and x_0 are the horizontal position of the plough and the surface vessel, respectively. By assuming that the plough's horizontal X-position is zero, the total length of the Catenary curve can also be found as follows:

$$s = a\sinh\left(\frac{x}{a}\right) \tag{2.92}$$

where x is the vessel's horizontal displacement in the inertial reference frame.

The Unstretched Towline Length

The unstretched length (L) of the towline is computed as the difference between total length (s) of the Catenary curve, from equation 2.92, and the stretched length (ΔL) due to tangential tension in the towline. According to Hook's law, ΔL can be computed as follows:

$$\Delta L = \frac{W}{K} \tag{2.93}$$

where $W = T \cdot g$ is the towline's tangential tension force as shown in Figure 2.21 and K is the towline's spring constant. g is the earth gravity constant. From Figure 2.21 it can be seen that the tangential tension (T) can be computed as follows:

$$W = \frac{T_0 \cdot g}{\cos(\theta_{cat})} \tag{2.94}$$

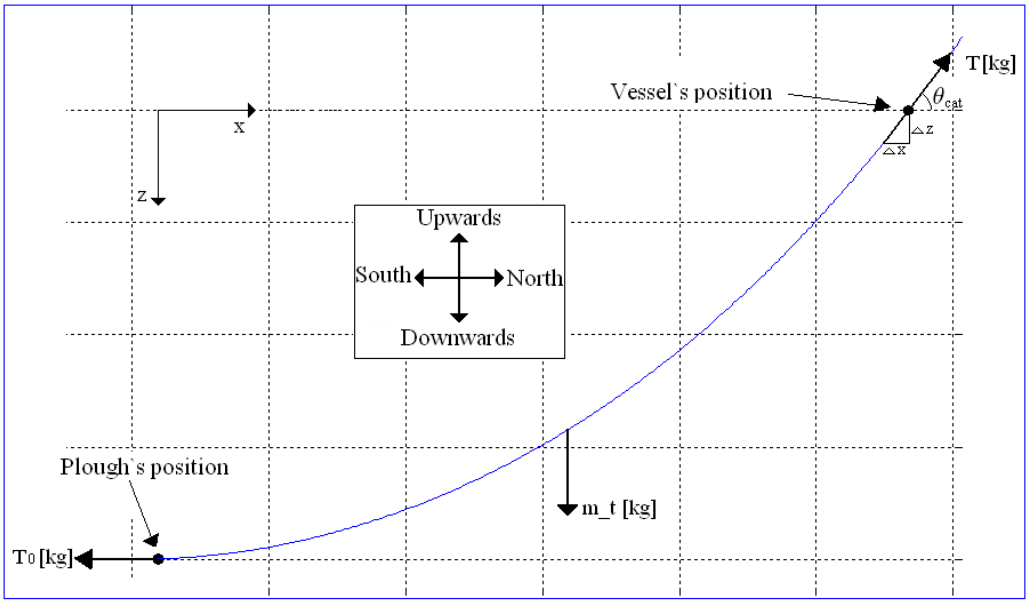

Figure 2.21: The shape of a Catenary curve.

where $\theta_{cat} = \arctan(\Delta z/\Delta x)$. The spring constant (K) is computed as follows:

$$K = \frac{E \cdot A}{L} \tag{2.95}$$

where E is the towline's elasticity modulus (Young's modulus), A is the towlines cross section and L is the towline's unstretched length. By combining equation 2.92, 2.93 and 2.95 the unstretched length of the towline can be expressed in the following form:

$$L = \frac{s}{\left(\frac{W}{E \cdot A} + 1\right)} \tag{2.96}$$

Experimental Initialization Procedure
An experimental procedure can be carried out in Simulink as follows:

- Define the ocean depth.
- Compute the Catenary curve from equation 2.89 and choose the towline's endpoints according to the endpoints of the Catenary curve.
- Compute the unstretched towline length (L) from equation 2.96
- Divide the the towline into n elements with equal length (L_e). The value of n depends on the ocean depth.

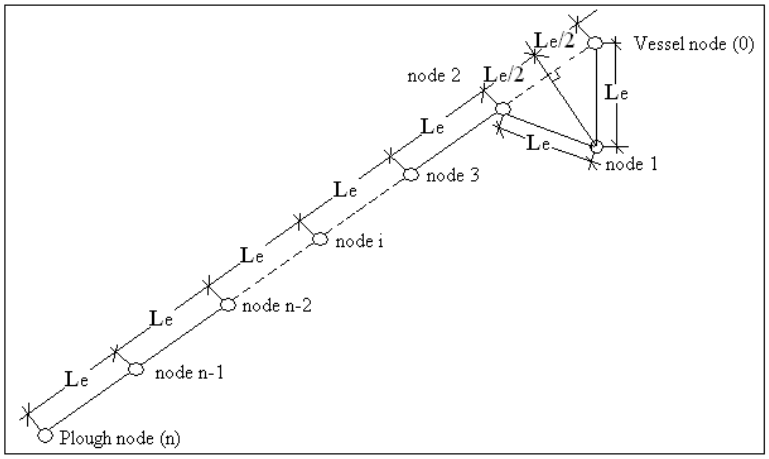

Figure 2.22: Manual placement of towline elements.

- Let the towline be drawn linearly between the end points. The first element node (node 1) below the surface vessel must be placed according to Figure 2.22. This is to maintain the unstretched length of the towline.
- Start the simulation and let it run until every towline element is at rest. The initial positions are now found.
- Start simulation of the ploughing operation.

Case Study of Initialization
In this case study the experimental initialization method described above is used to initialize the nodes position in the lumped mass model. The ocean depth (H_{sea}) is set to $200m$. This is, according to [22], a realistic ocean depth in the North Sea. According to [14], the towline model must consist of 20 to 30 towline elements when the ocean depth is set to $300m$. The number of elements is chosen to be $n = 25$. After simulating 100 seconds the lumped mass model of the towline, compared with the Catenary curve, gives the results shown in Figure 2.23. The blue curve is the towline's position at time zero. After about 100 seconds the towline (green curve) is at rest and it has approached the Catenary curve (red curve).

2.4.5 Discussion and Conclusions

The initialization of the towline in subsection 2.4.4 gave an adequate validation of the towline model. The towline approached the Catenary curve very well.

From the analysis in subsection 2.4.3, it can be concluded that the hydrodynamic drag has some damping effect on the towline's axial motion. But most of all it has a great damping effect on the towline's motion in the inertial reference frame (XZ-plane). The

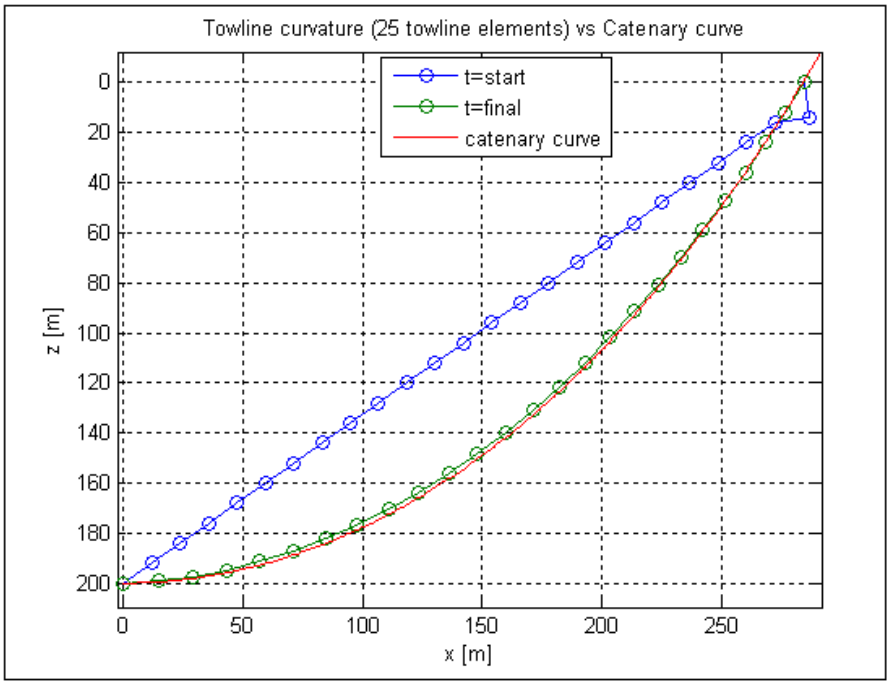

Figure 2.23: Experimental initialization of the towline elements vs the Catenary equation.

internal damping coefficient is hard to find and must be found experimentally. A coefficient has been chosen and will be used in the rest of the assignment.

The hydrodynamic drag coefficients are found to be functions of the Reynolds number, which again is a function of the tangential and normal speeds of the towline. This might be a problem if the equation of motion is to be evaluated analytically. The solution might be to linearize the equations about a desired speed and some desired towline angle.

Chapter 3

Control Design

Control design for marine vessels have been an active field of research for many years. Reference [11] introduces some modern control systems which have been successfully implemented on-board ships, underwater vehicles and floating vessels. This includes PID control system design, linear quadratic optimal control, state feedback linearizing and integrator backstepping.

In this chapter a dynamic positioning (DP) controller and a supervisor module will be derived for the surface vessel. The supervisor module will consist of a 3rd-order reference model that will be used to generate the desired vessel positions and a reference generator that will generate the vessel's reference values based on the plough's desired path. A short section on how to measure the system states are also introduced. A total system overview is shown in Figure 3.1.

3.1 Measurement Module

To measure the position, velocity and acceleration of an underwater plough, an Inertial Navigation System (INS) can be used in combination with a global positioning satellite system (GPS). However, the position of the plough can not be directly measured by the GPS since the plough is under water. Reference [6] gives a description on how an underwater towed vehicle can measure its position, velocity and acceleration by the use of INS and GPS measurement. The INS on board the underwater vehicle measures its acceleration. To estimate the velocity and position of the vehicle, this acceleration has to be integrated. Integration of INS measurements can result in unacceptable drifting of the position estimate. To prevent this drifting, it is common to use additional instrumentation. By transforming the position estimates of the surface vessel, provided by a GPS system, to the underwater vehicle, a combination of these estimates with INS measurements can be accomplished. By introducing a numerical model for the towline it is possible to transform the surface vessel position estimates to the underwater vehicle. The experiment in [6] gave promising numerical results, probably due to an exact knowledge on the mathematical model of the surface vessel. Due to this knowledge, the Kalman

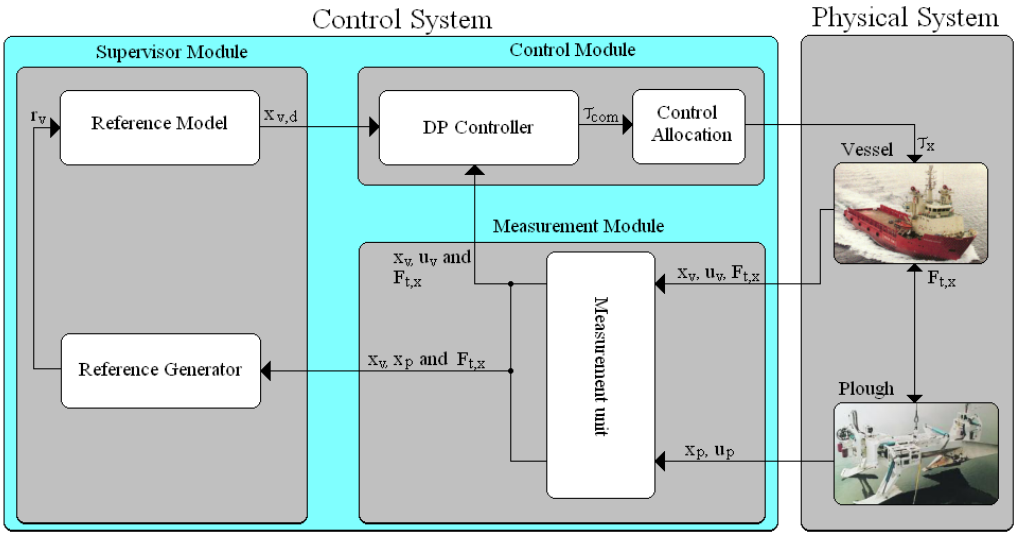

Figure 3.1: Total system overview.

filter gave good estimates of the vessel position and velocity. In a real situation, this will not be the case. Reference [9] gives a more detailed description on INS and GPS systems.

In this assignment it is assumed that the plough's and vessel's position and speed are measured without measurement noise. It is also assumed that the horizontal towline force is measured on board the vessel. This force can be measure by a tension measurement unit attached to a set of towline reels.

3.2 DP Controller

In this thesis the surface vessel model from equation 2.9 and 2.10, in chapter 2.2, will be equipped with a dynamic positioning (DP) controller. The DP control law is as follows:

$$\tau_x = F_{t,x} - K_p e - K_d u_v \qquad e = x_v - x_{v,d} \tag{3.1}$$

where $F_{t,x}$ is the horizontal force from the towline. This force is a varying bias term which has been assumed to be measured. When this force is perfectly known it can be implemented in the control law instead of having integral action. e is the position tracking error, x_v is the vessel's position, $x_{v,d}$ is the vessel's desired position and u_v is the vessel's surge speed. K_p is a proportional gain constant and K_d is a derivative gain constant. When combining equation 2.9, 2.10 and 3.1 the resulting equations becomes as follows:

$$\dot{x}_v = u_v \tag{3.2}$$

$$m_v \dot{u}_v + (K_d + d_v) u_v + K_p e = 0 \tag{3.3}$$

Equation 3.2 and 3.3 can be written in the following state space form:

$$\dot{\mathbf{z}}_v = \mathbf{A}\mathbf{z}_v + \mathbf{B}x_{v,d} \tag{3.4}$$

where $\mathbf{z}_v = \begin{bmatrix} x_v & u_v \end{bmatrix}^T$, $\mathbf{B} = \begin{bmatrix} 0 & \frac{1}{m_v} \end{bmatrix}^T$ and $\mathbf{A} = \begin{bmatrix} 0 & 1 \\ -\frac{K_p}{m_v} & -\frac{K_d+d_v}{m_v} \end{bmatrix}$.

To decide the gain constants K_p and K_d, the determinant for the closed system in equation 3.4 must be computed. This can be done as follows:

$$det(s\mathbf{I} - \mathbf{A}) = det\left(\begin{bmatrix} s & -1 \\ \frac{K_p}{m_v} & s + \frac{K_d+d_v}{m_v} \end{bmatrix}\right) = s^2 + \left(\frac{K_d + d_v}{m_v}\right)s + \frac{K_p}{m_v} \tag{3.5}$$

where $\mathbf{I}$ is a 2×2 diagonal identity matrix. The resulting 2nd-order polynomial must then be compared with the characteristic 2nd-order polynomial:

$$s^2 + 2\zeta\omega_n s + \omega_n^2 \tag{3.6}$$

where ω_n is the natural frequency for the closed system which must be chosen so that it becomes larger than the natural frequency for the surface vessel ($\omega_{n,v}$). ζ is the relative damping ration for the closed system. The closed system must be underdamped in order to keep track with the varying desired tracking position from the reference model to be derived in the next section. This means that the relative damping ratio ζ, from the characteristic 2nd-order polynomial, must be chosen to be:

$$\zeta < 1 \tag{3.7}$$

The gain constants K_p and K_d can be computed as follows:

$$K_p = \omega_n^2 m_v \tag{3.8}$$
$$K_d = 2\zeta\omega_n m_v - d_v \tag{3.9}$$

3.3 Supervisor Module

In the previous subsection a controller was derived in order to regulate the the vessel's position to a desired location. In this subsection a supervisor module, consisting of a reference model and a reference generator, will be derived, see Figure 3.1. The reference generator's assignment is to transform the plough's reference input into reference signals for the vessel. The reference model is needed to generate smooth and bounded desired tracking positions for the vessel from the reference model's input steps.

Reference Model

From [11] the following 3rd-order position and attitude reference model is found:

$$\frac{x_{v,d}}{r_v} = \frac{\omega_{n,r}^3}{s^3 + (2\zeta_r + 1)\omega_{n,r}s^2 + (2\zeta_r + 1)\omega_{n,r}^2 s + \omega_{n,r}^3} \tag{3.10}$$

where r_v is the vessel's reference position generated by the reference generator. $\omega_{n,r}$ is the natural frequency of the reference model, which must be chosen lower than the bandwidth of the vessel control system. ζ_r is the relative damping ratio.

A linear reference model has, according to [11], one drawback. The model's time constant can give one behavior for a certain input step while it can give a different behavior with another input step with a different amplitude. This is due to the exponential convergence of the signal in a linear system. One way to deal with this problem is to use amplitude gain scheduling so that the reference model design parameters $\omega_{n,r}$ and ζ_r are scheduled with respect to the magnitude of the input r_v. Another way to deal with this problem is to scheduling the input reference incrementally so that every step (r_v) has the same amplitude for a given set of $\omega_{n,r}$ and ζ_r. This last solution will be used in this assignment, and will be a task for the reference generator.

The performance of the reference model can be improved by including saturation elements for speed and acceleration. The saturation element is, according to [11], defined as:

$$sat(x_{v,d}) = \begin{cases} sgn(x_{v,d})x_{v,max} & \text{if } |x_{v,d}| > x_{v,max} \\ x_{v,d} & \text{else} \end{cases} \tag{3.11}$$

where the saturation limits:

$$u_{v,d} \leq u_{v,d}^{max} \qquad \dot{u}_{v,d} \leq \dot{u}_{v,d}^{max} \tag{3.12}$$

should reflect the physical limits of the vessel. This means that the vessel's speed can be bounded according to the maximum operational speed.

Reference Generator

Pipelines, which are to be buried into the seabed, are usually laid on the seabed before the ploughing/burial -operation begins. The ploughing path, in the XY-plane (horizontal plane), is therefore known in advance and can e.g be as shown in Figure 3.2. The red line in Figure 3.2 is the desired path. The plough must follow this path with the plough share directed toward the point where the path changes direction. In [11], this point is introduced as a way-point (reference point) given by the vessel's operator. Small perturbations from the desired path may damage the pipeline and it is therefore necessary to keep a low speed profile.

An algorithm called Line-Of-Sight (LOS) is introduced in reference [11] for solving this type of path following problem. The algorithm calculates of the plough's desired heading angle (ψ_{p_d}) and the point where the plough is switching to a new way-point. The plough's desired heading angle can be calculated as follows:

$$\psi_{p_d} = atan2(y_k - y_p(t), x_k - x_p(t)) \tag{3.13}$$

where $(x_p(t), y_p(t))$ is the plough's current position and (x_k, y_k) is the current way-point. The point where the plough must change to the next way-point is decided by the following

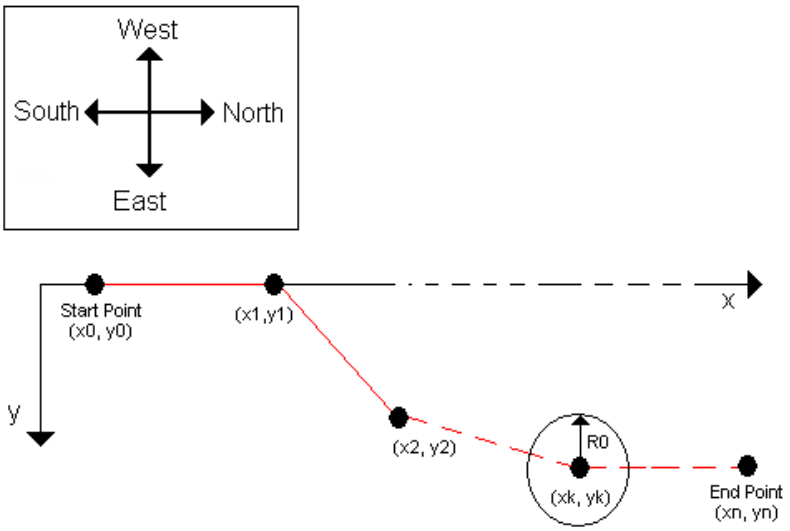

Figure 3.2: Ploughing path in the XY-plane (horizontal plane).

equation:

$$[x_k - x_p(t)]^2 + [y_k - y_p(t)]^2 \leq R_0^2 \tag{3.14}$$

where R_0^2 defines a circle of acceptance, see Figure 3.2.

In this assignment only the north-direction, along the X-axis of the inertial reference frame, is of interest, so it is assumed that the path is straight. The plough's desired path can be defined by a single desired position along the X-axis of the inertial reference frame.

As was described in subsection 2.4.4, it is known that when a chain or rope is loosely hung between two fixed points it hangs in a curve called a Catenary. This means that, when the vessel has a fixed X-position, the plough will converge to the X-position that will fit the Catenary curve's bottom position as shown in Figure 2.21. This is due to the unreleased potential energy in the towline. When the plough is at rest, the horizontal towline force is equal to the horizontal static force from the seabed sediment. The static sediment force, from equation 2.60 in chapter 2.3, is proportional to the sediment's density as shown in equation 2.21 in chapter 2.3. The Catenary curvature is dependent on this horizontal static force as shown in equation 2.89 in subsection 2.4.4. So if the sediment's density is known at the plough's desired position, the vessel's reference position can be calculated from equation 2.89 as follows:

$$r_v = r_p + \left(\cosh^{-1}\left(\frac{H_{sea}}{a} + 1\right)\right) \cdot a \tag{3.15}$$

where $z(x)$ in equation 2.89 is zero, r_v is the vessel's reference position, r_p is the plough's desired position set by the vessel's operator, H_{sea} is the ocean depth and a is the ratio

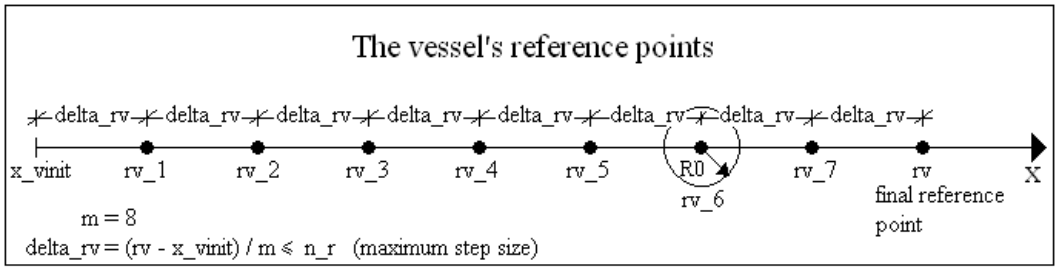

Figure 3.3: The vessel's reference points toward the final reference r_v.

between the plough's horizontal static force and the towline's weight pr. unit length.

As was discussed before, the reference model is vulnerable to different input step amplitudes. This can be solved by approaching the vessel's reference position (equation 3.15) incrementally. In other words; the reference r_v, in equation 3.15, must be divided into m smaller steps $delta_{rv}$ with a maximum amplitude n_r as shown in Figure 3.3. In this figure, $R0$ is the circle of acceptance where the vessel get a new reference point along the X-axis. $R0$ is defined as a percentage share of $delta_{rv}$. The algorithm for this approach is shown in Figure 3.4 and is implemented as an embedded MatLab function in the appended Simulink program for the total system, see appendix A.

If the plough should run into very hard seabed sediment, i.e. rocks, the towline will start building up a large tension. When this tension get large enough, the towlines's vertical force on the plough will exceed the weight of the plough and the plough will jump up from the seabed. This will cause great damage to the pipeline. In case the tension get larger than the maximum breaking load for the towline, the towline will break. To prevent this from happening, the vessel has to be stopped and if necessary reverse its motion direction. Due to the weight of the towline, the towline's vertical force will be largest on board the vessel. If this force can be measured, it can be used as a prewarning since the plough's submerged weight is known.

```
function rv   = fcn(r_p,x_p,x_pinit,x_v,x_vinit,a,Hsea,RO)
%------------------------------Defenitions---------------------------------%
% rv        Vessel's reference value.
% r_p       Plough's desired position.
% x_p       The plough's measured position.
% x_pinit   The plough's initial position.
% x_v       The vessel's measured position.
% x_vinit   The vessel's initial position.
% a         The ratio between the plough's static force and the towline's
%           weight pr. meter.
%Hsea       The ocean depth.
%RO         Circle of acceptance in percent of delta_rv.
%--------------------------------------------------------------------------%
n_r      = 10;                                      %Maximum step amplitude.
delta_rv = n_r+1;                                   %New reference step.
m        = 1;                                       %Number of smaller steps.

%Run while new reference step is greater that maximum step amplitude.
while delta_rv > n_r
    delta_rv = (r_p + a*acosh((Hsea/a)+1))/m; %Computing the new step size.
    if delta_rv <= n_r
        m = m;
    else
        m = m+1;
    end
end

r_v = x_vinit + delta_rv;              %The vessel's first reference value.

%Detecting when to increment the vessel's reference value by delta_rv.
for b=1:1:m-1
    %Testing if the vessel has reached the circle of acceptance.
    if x_v >= x_vinit + (b-RO)*delta_rv
        %Increment the vessel's reference value by delta_rv.
        rv = x_vinit + delta_rv*( b+1 );
    end
end
```

Figure 3.4: Transforming the plough's desired position into incremental reference step values for the vessel's position.

Chapter 4

Simulation and Results

4.1 How to Simulate the System in Simulink

In appendix A a CD can be found. On the CD there is a folder called "Ploughing Operation Sim". Open the Simulink model file "PloughingOperation" to start MatLab and then execute the following steps:

1 Open the file "Init1.m". Configure the data if necessary and run the file. Remember that the first thing this file does is to clear all data in the MatLab workspace.

2 Run the Simulink model file "PloughingOperation" as long as the timer is running. When the timer stops running, the towline is initialized and hangs like a Catenary curve.

3 Open the file "Init2.m" and run it. This file transforms the towline's current position into a new initial position vector, which will be used when simulating the ploughing operation.

4 One can now open the file "Plot.m" and view different figures or one can start simulating the total system by running the Simulink model file "PloughingOperation".

5 The Simulink model file "PloughingOperation" consist of three subsystems as can be seen when opening this file. By double clicking on the subsystems one can set different parameter for the simulation.

6 When a simulation is finished one can view the results by running the file "Plot.m".

7 When viewing figures where the inertial frame's Z-axis is involved, one should reverse this axis to get a correct picture.

8 If it is desired to change data in the file "Init1.m", one must repeat the steps 1 to 7 again.

Simulation data common for all case scenarios	Value
Ocean depth	H_{sea} =200m
Viscosity of seawater	μ_{sw} =0.0012$kg/(ms)$
Plough's submerged mass	m_p =52000kg
Vessel's mass and added mass	m_v =5.3122$e6kg$
Vessel's skin friction damping	d_v =5.0242$e4kg/s$
Number of towline elements	n_e =25
Towline's internal damping coefficient	C_v =8980kg/s
The surface vessel's initial position along the X-axis	$x_{v,init}$ =0m
The plough's initial position along the X-axis	$x_{p,init}$ =$-284.75m$
Proportional controller gain	K_p =359104.72
Derivative controller gain	K_d =2159633.2
Natural frequency for the reference model	$\omega_{n,r}$ =0.09
Relative damping ratio for the reference model	ζ_r =2.5
Speed saturation limit in the reference model	u_{max} =0.1m/s
Maximum input step size to the reference model	n_r =10m
Plough and seabed sediment data from Table 2.1	
Towline data from Table 2.2	

Table 4.1: Simulation data common for all case scenarios.

4.2 Simulation Data

In this chapter different case scenarios will be simulated with a set of system parameter data. The simulation data that are common to all cases are shown in Table 4.1.

The DP-controller gain constants K_p and K_d from equation 3.9 in chapter 3, and their values defined in Table 4.1, are based on the natural frequency $\omega_n = 0.26$, which is chosen larger that the vessel's natural frequency, and the chosen relative damping ratio $\zeta = 0.8$. This result in the following complex eigenvalues: $\lambda_1, \lambda_2 = -0.208 \pm 0.156 \cdot i$. This means that the closed system is asymptotically stable and that the controller is able to regulate the vessel to a desired position within a bounded time period.

The natural frequency for the reference model in the supervisor module is chosen to be $\omega_{n,r} = 0.09$. It is chosen smaller than the one for the closed system because the closed system must be able to track the desired vessel position generated by the reference model. The relative damping ratio for the reference model was chosen to be $\zeta_r = 2.5$. This gives a smooth overdamped desired vessel position ($x_{v,d}$).

4.3 Simulation Case 1: Perfect Operational Conditions

In this case there are no underwater currents involved. Different sub cases will be performed to expose how the ploughing operation behavior changes with different values

for the circle of acceptance ($R0$) in the reference generator model and with different values for the plough's desired position (r_p).

4.3.1 Operational Behavior Over a Short Distance Whit Different Circle of Acceptance

In this sub case the operational behavior is simulated when $R0 = 0$ and when $R0 = 0.25$. In both cases the desired plough position is $r_p = -250m$, which means that the plough must be moved $34.75m$ along the X-axis in the positive direction.

Results
In Figure 4.1 and 4.2 the vessel's and the plough's positions are plotted with different circle of acceptance ($R0$). In the case where $R0 = 0$ the vessel converges to the different reference points (red line) along the path to the desired location. When $R0 = 0.25$ the vessel gets a new reference position before it reaches its current reference. This results in a smooth motion for the vessel. In both cases, the plough reaches its desired position in a relatively smooth manner. The vessel follows its desired position signal, generated by the reference model, quite well although there is a small deviation due to the ramp function of the desired position signal. This deviation could be reduced by increasing the closed system's natural frequency.

In Figure 4.3 and 4.4 the vessel's and the plough's speed is plotted. In the case where $R0 = 0$ the plough's speed is gradually increasing, and the vessel stops after every reference convergence. For $R0 = 0.25$ the plough's speed increases smoothly due to the vessel's continuous speed. On such short distances the plough's speed will never gain the same amplitude as the vessel's. It is seen that the vessel's speed has a maximum value $u_v = 0.1m/s$ which is due to the saturation limit in the reference model.

In Figure 4.5 and 4.6 the vessel's control force and the horizontal towline force at each end of the towline is plotted. It can be seen that the horizontal towline force is the same at both ends of the towline. Only in the beginning of the simulation there is a small difference. This is due to different oscillations in the towline elements caused by the vessel's acceleration. If the towline is exposed to an underwater current, there will be a greater difference between the two end nodes horizontal force. The difference between the forces when $R0 = 0$ and when $R0 = 0.25$ can be explained from the speed plots.

In Figure 4.7 and 4.8 the towlines's elongation is plotted. In the case where $R0 = 0$ the towline has a maximum elongation of about $14m$. This is 3.94% of the unstretched towline length. When $R0 = 0.25$ the towline elongates with about $19m$, which is 5.35% of the unstretched towline lengt.

As a conclusion to this simulation case it can be said that the circle of acceptance should be larger than zero to avoid jerkily motion of the plough and to avoid large oscillations in the towline.

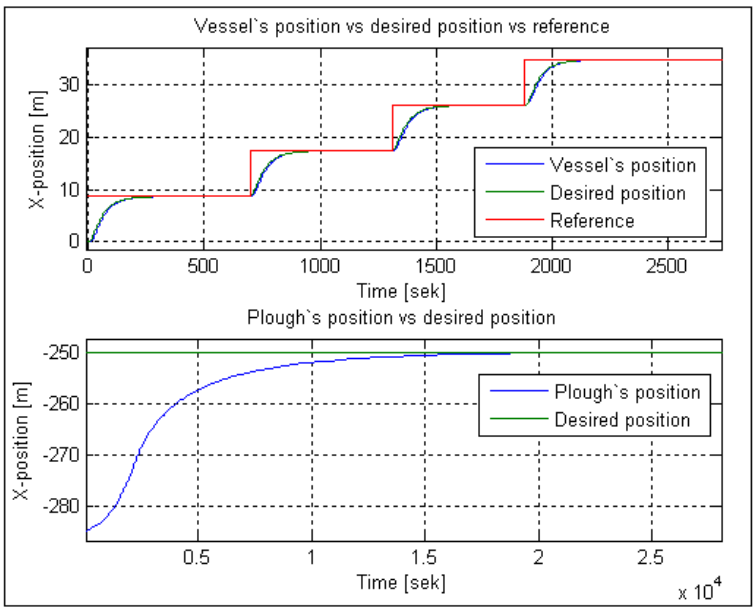

Figure 4.1: The vessel's and plough's position vs their desired position and reference ($R0 = 0$ and $r_p = -250m$).

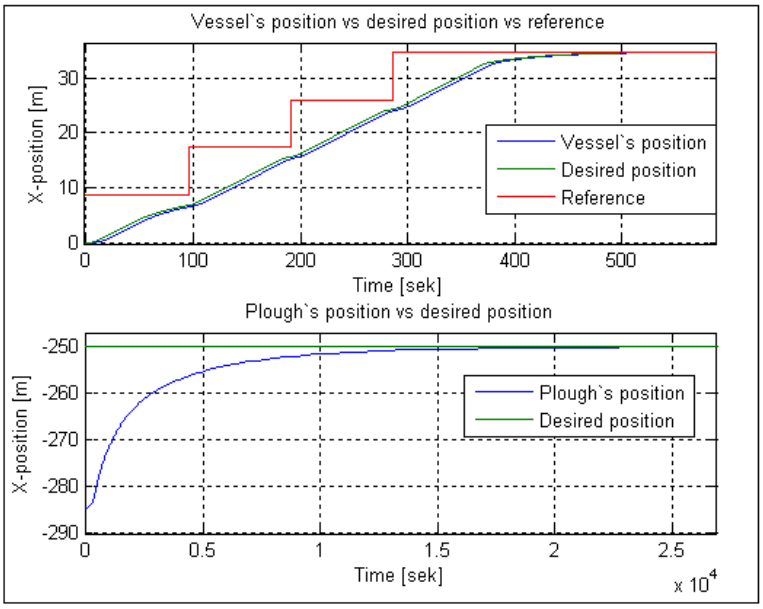

Figure 4.2: The vessel's and plough's position vs their desired position and reference ($R0 = 0.25$ and $r_p = -250m$).

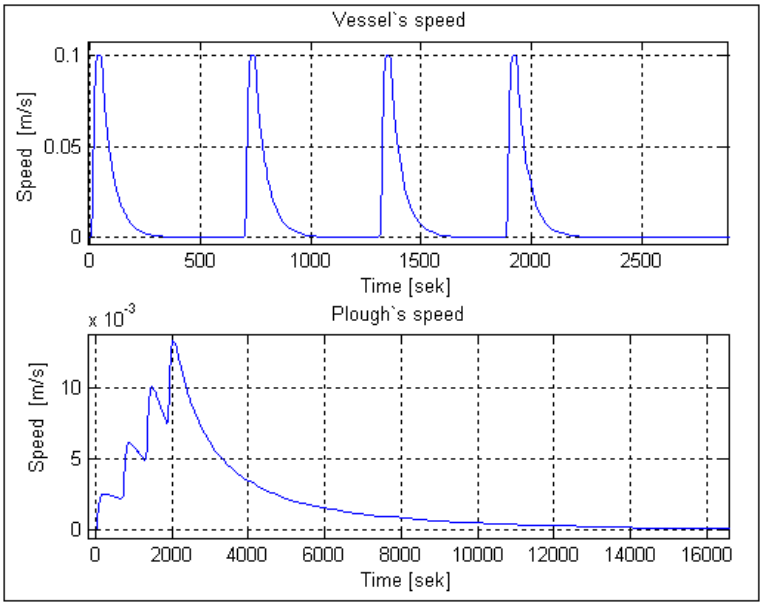

Figure 4.3: The vessel's and plough's speed ($R0 = 0$ and $r_p = -250m$).

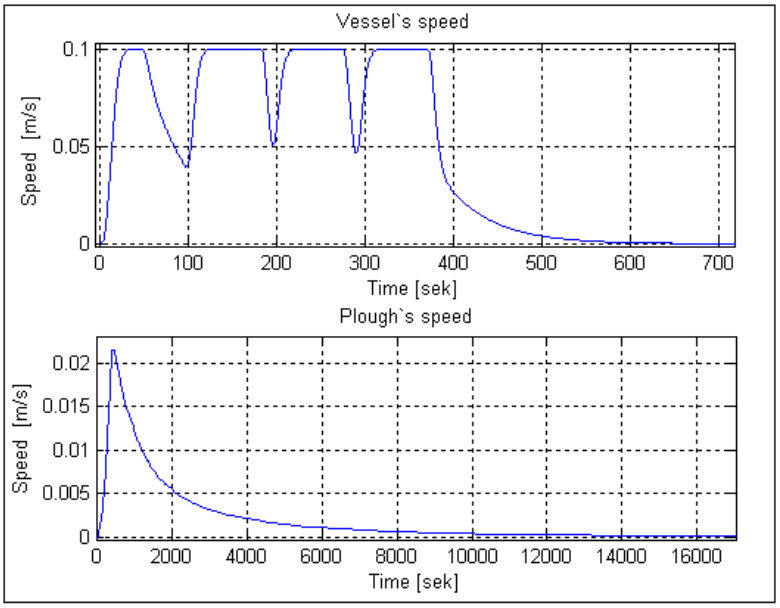

Figure 4.4: The vessel's and plough's speed ($R0 = 0.25$ and $r_p = -250m$).

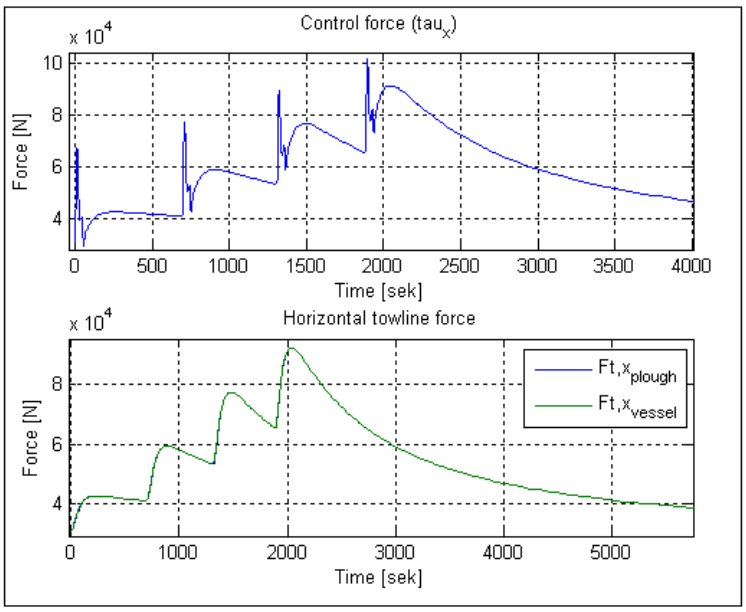

Figure 4.5: Control force and horizontal towline forces ($R0 = 0$ and $r_p = -250m$).

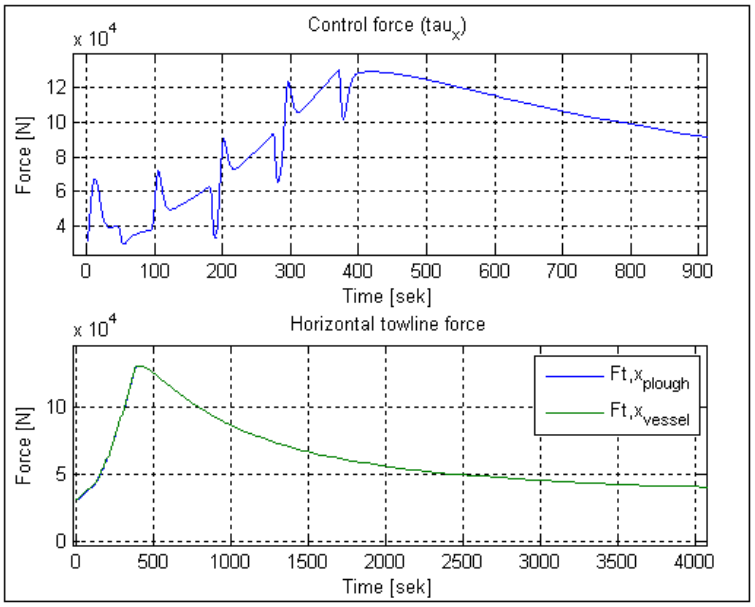

Figure 4.6: Control force and horizontal towline forces ($R0 = 0.25$ and $r_p = -250m$).

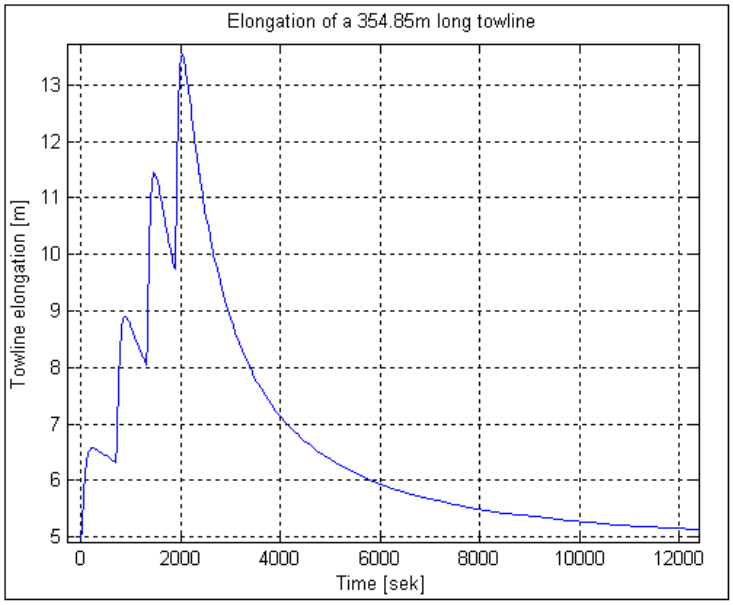

Figure 4.7: Elongation of the towline ($R0 = 0$ and $r_p = -250m$).

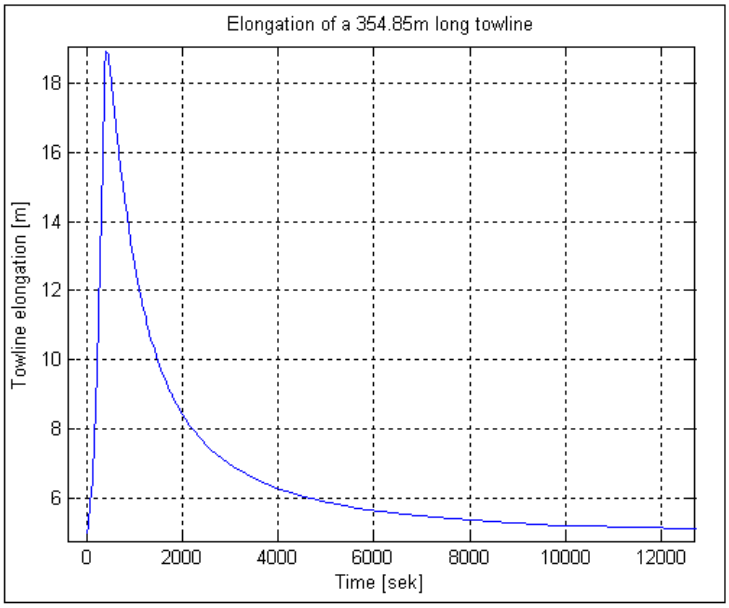

Figure 4.8: Elongation of the towline ($R0 = 0.25$ and $r_p = -250m$).

4.3.2 Operational Behavior Over a Longer Distance

In subsection 4.3.1 the plough was moved over a small distance with two different circle of acceptance. The choice of $R0 = 0.25$ gave smooth desired tracking positions for the vessel's control system and the plough's speed was much smoother than when choosing $R0 = 0$. In this subsection the desired plough position is changed to $r_p = 0m$ which means that the plough must be moved $284.75m$ along the X-axis in the positive direction. The circle of acceptance is chosen to be $R0 = 0.25$.

Results
In Figure 4.9 the vessel's and the plough's positions are plotted. It can be seen that the vessel reaches its final reference value after about 2850 seconds. At this time, the plough has reached about 65% of its final destination. The weight of the towline provides for the next 35%. This is due to the unreleased energy in the towline. The plough converges to the desired position after about foure hours.

In Figure 4.10 the vessel's and the plough's speed is plotted. It can be seen that the vessels's speed increases fast up to $u_v = 0.1m/s$ and stays at this speed until it has reached its final reference. The plough's speed u_p is increasing much slower and approaches the vessel's speed. When the vessel's and the plough's speed is the same, the horizontal towline force becomes constant as shown in Figure 4.11. This also result in that the towline no longer elongates as shown in Figure 4.12. The towline elongation in this figure is about 17% of the unstretced towline length. The horizontal towline force increases up to a constant value of $450kN$, when the ploughing speed is $0.1m/s$. This force reflects the seabed sediment force in Figure 2.14 in subsection 2.3.4.

In Figure 4.13 the system's initial and final states are shown. The blue curve is the initial position for the plough, the towline elements and the vessel. The green curve is their final position which converges to the Catenary curve (red curve).

As a conclusion to this simulation case it can be said that the vessel's speed is kept at the maximum value over a longer period of time when crossing longer distances. This gives a time efficient operation, and wear and tear of the propulsion system is avoided.

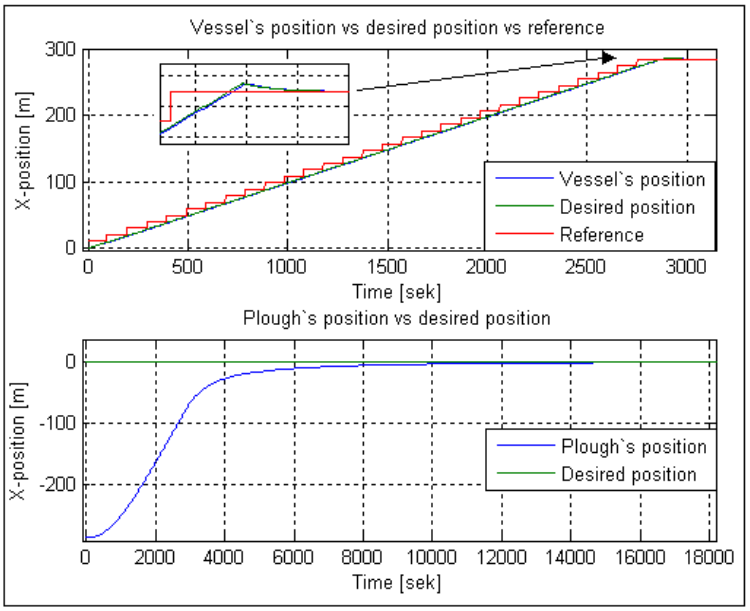

Figure 4.9: The vessel's and plough's position vs their desired position and reference ($R0 = 0.25$ and $r_p = 0m$).

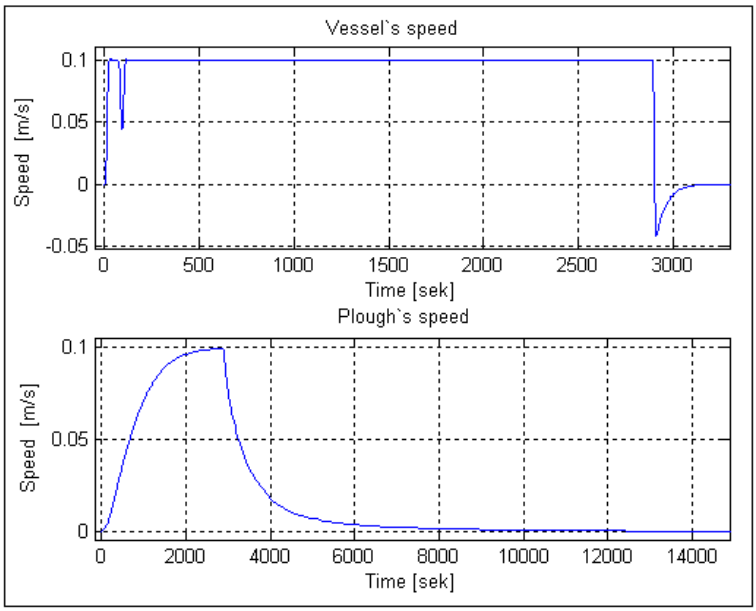

Figure 4.10: The vessel's and plough's speed ($R0 = 0.25$ and $r_p = 0m$).

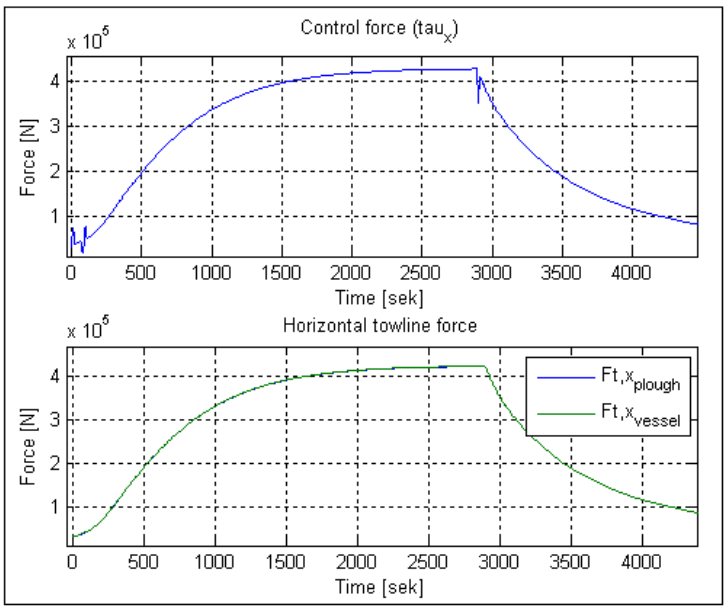

Figure 4.11: Control force and horizontal towline forces ($R0 = 0.25$ and $r_p = 0m$).

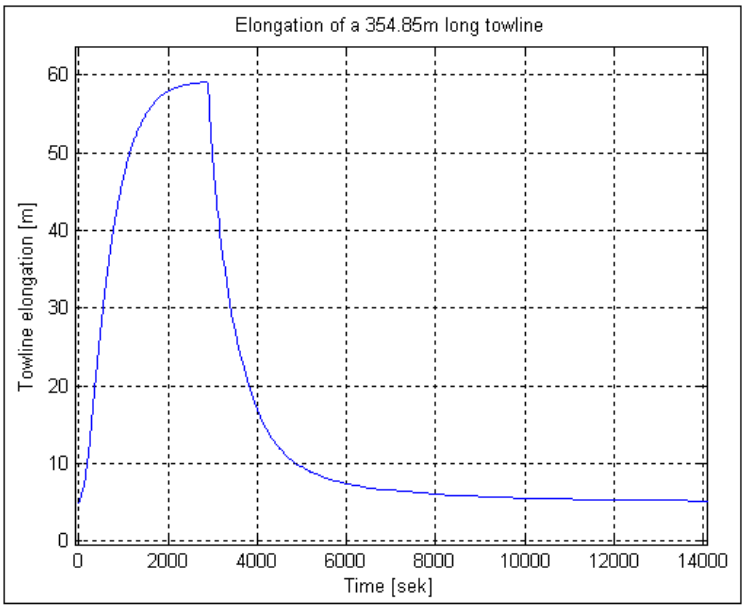

Figure 4.12: Elongation of the towline ($R0 = 0.25$ and $r_p = 0m$).

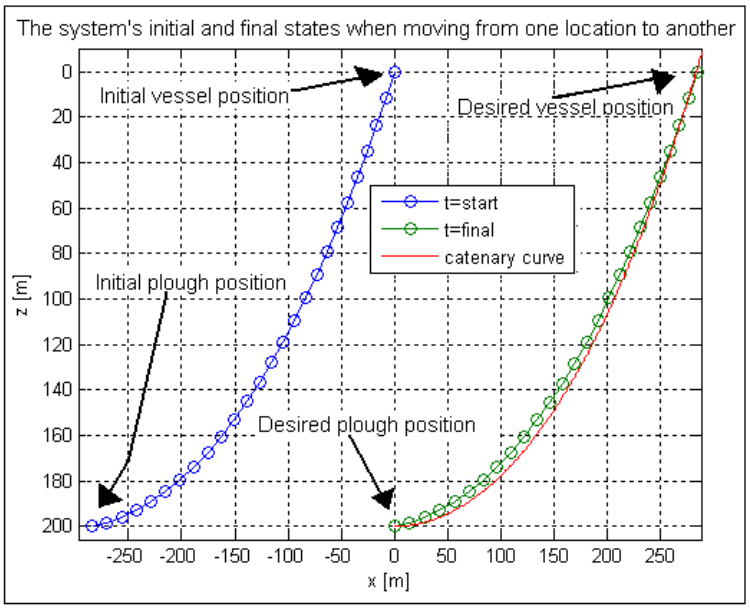

Figure 4.13: The system's initial and final states ($R0 = 0.25$ and $r_p = 0m$).

4.4 Simulation Case 2: Operational Behavior When the Towline is Exposed to Underwater Current

In this section the towline elements are exposed to an underwater current with speed $U_x = 0.9m/s$ in the north direction, see Figure 2.17 in subsection 2.4.1. The circle of acceptance is $R0 = 0.25$ and the plough's desired position is $r_p = -250m$.

A simulation case has been performed in addition to this where the plough's desired position was set to $r_p = 0$. This case gave almost the same results as in subsection 4.3.2 because the large towing forces suppressed the hydrodynamic forces from the seawater current. In this case, with the results described below, the plough's speed is low due to the short distance from the desired position.

Results

When comparing Figure 4.14 with Figure 4.6 it can be seen that the underwater current has great influence on the towline when the speed is low. When using the towline's horizontal force as feed forward in the DP controller this can give noisy command signal to the propulsion system. As can be seen from Figure 4.14 is that the control force τ_x is almost free from noise. This is because a 1st order low-pass filter is implemented in the controller to damp out the towline's high frequencies. The position and speed plots are not of interest in this case simulation since they are almost similar to previous simulation results.

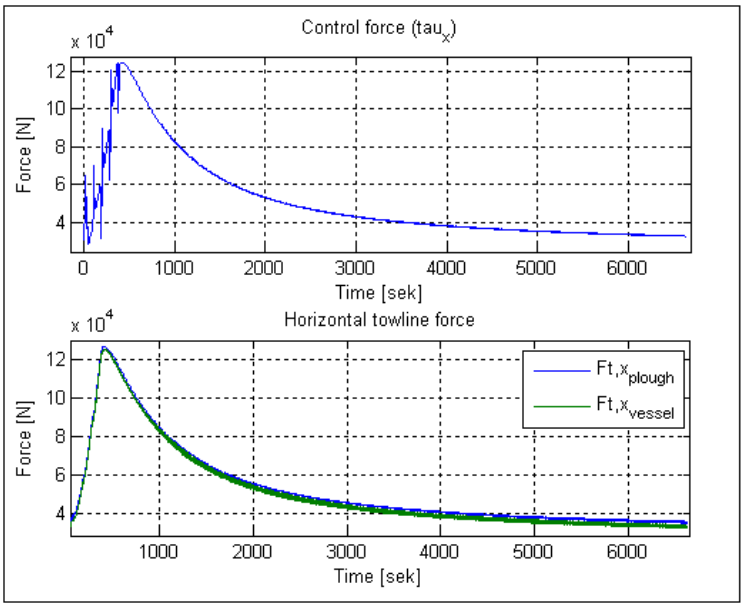

Figure 4.14: Control force and horizontal towline forces (with underwater current).

Chapter 5

Discussion and Conclusion

During this thesis work, mathematical models required to simulate an offshore ploughing operation has been derived. Three models have been required; a surface vessel model, a model of the plough and its friction force due to seabed sediment and a towline model. A Dynamic Positioning control system has been derived in order to regulate the vessel to a desired location based on the plough's desired position. A supervisor module has been derived in order to generate the vessel's reference position in a smooth manner. And finally the total system has been implemented and simulated in the Simulink_TM environment.

The surface vessel model derived in this assignment is based on an offshore supply vessel from the "MatLab Marine GNC Toolbox" in Simulink_TM. This type of vessel is not designed to perform towed pipeline ploughing operations. Much larger and heavier vessels are required for such operations. But for simulation reasons this model is adequate. The vertical motion of the vessel has been kept constant during simulations, based on the assumption that the buoyancy force of the vessel is large compared to the vertical towline force. Implementation of the vessel's vertical motion is proposed as future work. It is also proposed that the "MatLab Marine GNC Toolbox" should be extended to contain vessel models suited for ploughing operations.

The plough's friction force due to penetration of the seabed sediment has been modeled, based on the content in reference [5], to get a realistic picture of the sediment forces involved in ploughing operations. It was found that the plough's friction force profile changed with different operational boundaries. The boundaries are the ocean depth and the ploughing speed. For the boundaries in this assignment the resulting ploughing force equation were found to be nonlinear and shaped as a sigmoid function. The equation consists of a speed dependent part and a static part.

In the North Sea many types of sediment can be involved during a single operation, but the most common is clay. In this assignment, data on Nevada sand has been available and used in case studies. This type of sediment is lightweight compared to clay so the

forces, when penetrating clay, should be much larger. The seabed sediment parameter in the ploughing force equation is not always easy to find for different type of sediment, but should be predicted so that they reflects the essential force profile and magnitude.

Towlines are also called cables. Mathematical modeling of a towline can be performed by using one of several methods. The method used depends on i.e the type of computer control system used. The lumped mass method used in this assignment is a simple method which gives reasonably good numerical results when implemented in the Simulink_TM environment. To get a realistic towline motion in seawater, a hydrodynamic quadratic damping force must be added to the equations. This hydrodynamic damping has effect on the towline's tangential and normal motion components. The tangential component has the same effect as the internal damping force. Internal damping coefficients are usually difficult to find for towline cables but can be replaced by an additional hydrodynamic linear damping part.

The DP controller derived in this assignment consists of a PD-controller with feed forward signal from the horizontal towline tension. Instead of this feed forward signal an integrator could have been used to compensate for the horizontal towline force and other bias terms that might occur. Feed forward signals are often influenced by noise and must be filtered to obtain low-frequency signals. In this assignment a ordinary 1st-order low-pass filter has been used in order to damp out oscillations from the towline. From the simulations in chapter 4 it can be concluded that this had a nice effect. It can also be concluded that the controller has a very good position tracking quality.

The supervisor module designed in chapter 3 is responsible for converting input signals for the plough's desired position/path into a smooth tracking signal for the vessel's control system. A reference generator produces smaller intermediate reference signals, as input to a reference model, from a final desired vessel position. These intermediate reference signals has equal amplitudes based on the chosen parameters in the reference model. A circle of acceptance has been introduced in order to change reference values at a convenient vessel location. It can be concluded that this had a nice effect on the vessel's and the plough's behavior when chosen to one quarter of the intermediate reference value. The reference model has been designed with a speed saturation element in it. It can be concluded that this saturation element gives good results since the vessel's speed could be bounded to a speed which is reasonable for ploughing operations.

The reference generator has one drawback. The seabed density has to be known at the plough's desired position/location. This is because the Catenary equation, which is dependent on the horizontal static sediment force, decides the distance between the plough and the vessel when they are in steady state. A further look into this model is proposed as future work.

It can be concluded from the simulation results in chapter 4 that by defining the op-

eration over a longer distance, a more efficient operation is gained. This is partially because, when the vessel has reached its desired position, the weight of the towline is responsible for moving the plough its final distance. This is a time consuming process and should not be done to often during an operation. When crossing longer distances the plough will reach the vessel's speed of $0.1m/s$. And at this speed, underwater current disturbances are small compared to the ploughing force. Underwater currents has great influence on the towline when the speed is low.

From one of the simulation cases in chapter 4 it can be found that the towline's axial elongation was 17% of the unstretced towline length. This is because the steel wire used in this assignment follows Hook's law, from equation 2.93, at all times. In real life, this law is only valid for a limited elongation, depending on the towline type, due to physical boundaries. The towline model implemented in the simulator in this assignment has no limits. Implementing elongation limits is proposed as future work.

The ploughing operation modeled and simulated in this assignment is bounded to the vertical XZ-plane. For future work this can be extended to also account for the horizontal XY-plane.

Bibliography

[1] O.M. Aamo and T.I. Fossen. Finite element modeling of moored vessels. In *Math. Comput. Modelling Dynamical Syst.*, number 7(1), pages 47–75, 2001.

[2] ScanRope AS. Wire ropes. *Data sheet*, 2003.

[3] M.F. Bransby, G.J. Yun, D.R. Morrow, and P. Brunning. The performance of pipeline ploughs in layered soils. In *Offshore Geotechnics: ISFOG 2005*, pages 597–606, 2005.

[4] Catenary equation. http://www.offshoreengineering.org/moorings/2005/catenaryb/theory.html, 16.May, 2007.

[5] J.C. Coyne and G.W. Lewis. Analysis of plowing forces for a finite-width blade in dense, ocean bottom sand. In *proceedings of OCEANS '99 MTS/IEEE, Seattle, WA, USA*, pages 1–10, 1999.

[6] G. Damy, M. Joannides, F. LeGland, M. Prevosto, and R. Rakotozafy. Integrated short term navigation of a towed underwater body. In *proceedings of Oceans '94, Brest, France*, 1994.

[7] D.Bray. Dynamic positioning. *Oilfield Publications Limited*, 2003.

[8] R. Driscoll and M. Nahon. Mathematical modeling and simulation of a moored buoy system. In *proceedings of Oceans 96*, number 1, pages 517–523, 1996.

[9] J.A. Farrell and M. Barth. *The Global Positioning System and Inertial Navigation.* McGraw-Hill, New-York, 1998.

[10] T. I. Fossen. A nonlinear unified state-space model for ship maneuvering and control in a seaway. *International journal of bifurcation and chaos in applied sciences and engineering*, 15(9):2717–2746, 2005.

[11] T.I. Fossen. *Marine Control Systems, Guidance, Navigation, and Control of Ships, Rigs and Underwater Vehicles.* Marine Cybernetics, 2002.

[12] T.I. Fossen and J.P Strand. Passive nonlinear observer design for ships using lyapunov methods: full-scale experiments with a supply vessel. *Automatica, Oxford*, 35(1):3–16, 1999.

[13] Jespersen. ScanRope Marine AS, Tønsberg, Norway. Personal contact, 2007.

[14] Vegar Johansen. SINTEF, Trondheim, Norway. Personal contact, 2007.

[15] Modular plough system (mps) pipeline mode specifications. http://www.ctcmarine.com, 10.April, 2007.

[16] Ormen lange. http://www.hydro.com, 7.May, 2007.

[17] Petter Ottesen. ODIM AS, AAlesund, Norway. Personal contact, 2007.

[18] Professor Eilif Pedersen. Department of Marine Technology , NTNU, Trondheim, Norway. Personal contact, 2007.

[19] D. Perrault, G. Hackett, and M. Nahon. Simulation and active control of towed undersea vehicles. In *proceedings of OCEANS '97, Halifax, NS, Canada*, pages 1277–1282, 1997.

[20] Kostnadsanalyse av ulike disponeringsalternativ for utrangerte rørledninger og kabler. http://www.regjeringen.no/oed/html/rapporter/11, 18.May, 2007.

[21] F.C. Teixeira, A.P. Aguiar, and A.M. Pascoal. Nonlinear control of an underwater towed vehicle. In *proceedings of the* 6^{th} *IFAC MCMC, Lisbon, Portugal*, 2006.

[22] Captain Tor Helge Tjøsvoll. Solstad Shipping A/S, Skudeneshavn, Norway. Personal contact, 2007.

[23] M. Toda. A theoretic analysis of a control system structure of towed underwater vehicles. In *proceedings of the* 44^{th} *IEEE Conference, Decision and Control and European Control Conference*, pages 7526–7533, 2005.

[24] P.H. Wang, R.F. Fung, and M.J. Lee. Finite element analysis of a three-dimensional underwater cable with time-dependent length. *Journal of sound and vibration*, 209(2):223–250, Juli 1998.

Appendix A

CD

The content on the CD is sorted into different folders as shown in Figure A.1.

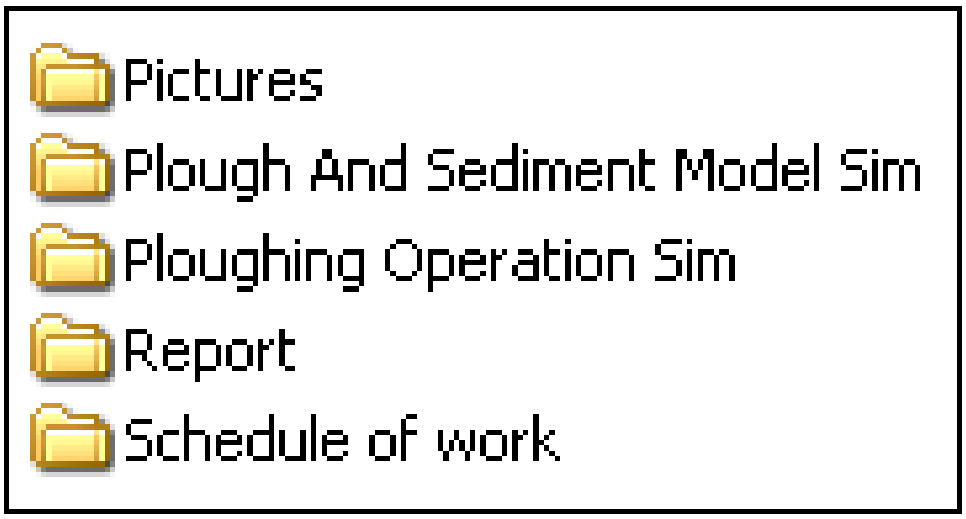

Figure A.1: CD content.